VILNIAUS UNIVERSITETAS

CHEMIJOS IR GEOMOKSLŲ FAKULTETAS

CHEMIJOS FAKULTETAS

NEORGANINĖS CHEMIJOS KATEDRA

Adolfas Žukauskas

Pagrindinių studijų programa Chemija – 2 kursas

Search for and Characterisation of Binders for Composite Aqueous Sodium-Ion Batteries

Magistro studijų baigiamasis darbas

Darbo vadovas: Dr. Doc. Jurgis Pilipavičius,

Konsultantė :Nadežda Traškina,

Įvertinimas:

_____

(Data, įvertinimas, parašas)

Vilnius, 2026

TABLE OF CONTENTS

LIST OF ABBREVIATIONS

CB - Carbon black

CMC - Carboxymethyl cellulose

CV - Cyclic voltammetry

EVA-SIS - Ethylene vinyl acetate - styrene Isoprene Styrene

GCD - Galvanostatic charge/discharge

HER - Hydrogen evolution reaction

HIDTPO - 4-hydroxy-6-isopropyl-5,5-dimethyl-tetrahydro-pyrimidin-2-one

LA81 - Laropal A81

LIB - Lithium-ion battery

LMO - Layered metal oxides

MMA-BA - Methyl methacrylate-butyl acrylate

NASICON - Na super ionic conductors

NMP - N-Methyl-2-pyrrolidone

NTP - Sodium titanium phosphate

NVTP - Sodium Vanadium Titanium Phosphate

OER - Oxygen evolution reaction

PB44 - Paraloid B-44

PB48 - Paraloid B-48

PB67 - Paraloid B-67

PB72 - Paraloid B-72

PBA - Prussian blue analogues

PGPQ - Plexigum PQ611

PIBMA - PolyIsobutyl methacrylate

PMMA-EA polymethyl methacrylate-ethyl acrylate

PVA - Pol(yvinyl alcohol)

PVB - Poly(vinyl butyral)

PVDF - Poly(vinylidene difluoride)

RR1125 - Regolite R1125

SHE - Standard hydrogen electrode

SIB - Sodium-ion battery

UIF - Urea–isobutyraldehyde–formaldehyde

XRD - X-ray diffraction

INTRODUCTION

In recent decades, in an attempt to meet the massive energy demand without further damaging the environment, renewable energy sources have been widely used, and due to their limited operating time, stationary batteries have been employed in parallel. The purpose of these devices is to store electrical energy as efficiently as possible in terms of cost and energy, and sodium-ion batteries can achieve this because sodium is widely distributed in nature and inexpensive. Aqueous sodium-ion batteries are especially attractive due to their inexpensive electrolytes, yet they face many challenges, as conventional electrodes, and especially their binders, are not compatible with aqueous solutions and, in many instances, are unusable.

The main goal of this work is to prepare cast electrodes for aqueous sodium-ion batteries using a variety of potential binders compatible with aqueous electrolytes and to compare their performance with conventional poly(vinylidene) difluoride-based electrodes.

In order to reach this goal, these objectives were set:

1) To prepare electrodes using alternative binders for sodium ion batteries, evaluate their compatibility with aqueous electrolyte solutions and choose the most optimal binders for further electrochemical evaluations.
2) To evaluate the alternative binder containing electrode electrochemical performance both in positive and negative electrodes, and compare to conventional poly(vinylidene) difluoride-based electrodes.
3) To compare the electrode surface defects post-electrochemical activity in order to better understand their performance and to choose the optimal binder.

1. LITERATURE OVERVIEW

1.1 Batteries

Batteries are devices in which chemical energy is converted into electrical energy through redox reactions. Batteries usually consist of a positive electrode, a negative electrode, a separator separating them, an electrolyte, current collectors, and an outer casing (Fig. 1). A battery electrode is typically a composite film, primarily made up of an active material, that participates in redox reactions, an electrically conductive additive and a binder that ensures cohesion between the remaining components and the current collector. During battery discharge, the negative electrode active material is oxidised, and the electrons travel through the external circuit to the positive electrode, where its active material is reduced.[1] The main parameters used to describe batteries are battery capacity, energy density and capacity retention. Battery capacity indicates the amount of charge the electrode can store and deliver under specified charge - discharge conditions. Energy density refers to the amount of energy a battery can store per unit weight. Capacity retention measures how much capacity the battery retains over its lifetime compared to its initial capacity.[2],[3]

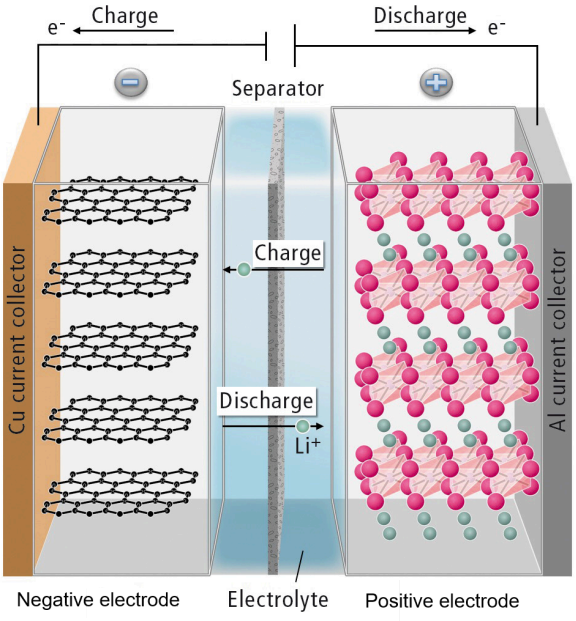

Figure 1. A scheme of a lithium-ion battery.[4]

Depending on the reversibility of the redox reactions occurring in batteries, they can be primary (disposable) or secondary (rechargeable). Currently, environmental and economic challenges drive demand for secondary batteries, the most well-known being the lithium-ion battery (LIB). LIBs became commercially available in the 1990s and, due to their high theoretical capacities, high energy density, and low reduction potential (-3.04 V vs standard hydrogen electrode (SHE)), have established themselves as the dominant technology to this day. The principle of operation of these batteries is based on the reversible intercalation of Li ions into electrodes. As the battery discharges, the negative electrode is oxidised and releases electrons, which travel through an external circuit to the positive electrode, which is reduced, creating an electric current. At the same time, lithium ions travel through the separator from the negative electrode to the positive electrode to maintain charge neutrality. The reverse process occurs during charging. [5] Many possible LIB systems are detailed in the literature, but the most popular ones are graphite as the negative electrode and $Li[Ni_xCo_yMn_z]O_2$, $LiFePO_4$, or $LiMn_2O_4$ as the positive electrode. The range of theoretical capacities of these batteries with organic electrolytes is 120-300 mAh/g. [6][7]

Despite their clear advantages, LIB technologies are nearing their development limits, with energy densities approaching 300 Wh/kg. Also, the intensive use of lithium is straining its supply and driving up battery prices. Another fact worth noting is that accidents involving flaming batteries in mobile phones, computers, and electric cars have led to an increased focus on safety in the development of new batteries. Further progress in these technologies requires alternative, innovative solutions and the search for new materials and electrolytes. [5][8]

1.2 Sodium ion batteries

Sodium, being one of the most abundant elements in the Earth's crust, is more easily extracted and processed than lithium. This, in turn, leads to a greatly reduced price of sodium-ion battery (SIB) raw materials compared to LIBs. The battery price is further reduced by opting for aluminium current collectors instead of the expensive copper, as aluminium cannot be used with lithium due to alloying. Also, eliminating enables simplified transport and storage of fully discharged SIBs [9]. SIBs are also advantageous in terms of safety, as they withstand higher temperatures, physical damage or overcharging before thermal runaway begins.[3][9] Despite these advantages, SIBs have not been as extensively studied as LIBs because the larger ionic radius and higher molar mass of sodium ions result

in a lower theoretical capacity.[10] Various SIBs with capacities ranging from 80 to 220 mAh/g have been reported in the literature. The lower theoretical capacity reduces the prospects of applying this technology to mobile devices. Still, it does not prevent its use in stationary energy-storage systems for renewable sources, where battery size is less of a concern. [11]

1.3 Aqueous sodium ion batteries

. Commercial SIBs typically use sodium salts such as $NaClO_4$, sodium bis(trifluoromethanesulfonyl)imide) or $NaPF_6$ dissolved in organic solvents such as ethylene carbonate, dimethyl carbonate, and propylene carbonate as their electrolyte solutions.[12] Different from their lithium counterparts, SIBs are compatible with safer, more environmentally friendly aqueous electrolytes based on simple salts such as Na_2SO_4, $NaNO_3$, $NaClO_4$, and others. These salts are common, harmless to humans and the environment, and inexpensive both in terms of purchase and disposal. One of the main disadvantages of aqueous electrolytes is a narrow electrochemical stability window (about 1.2 V), beyond which the hydrogen evolution reaction (HER) and oxygen evolution reaction (OER) occur, leading to rapid battery degradation.[13] Another disadvantage is the need for an alternative negative electrode material. Graphite, which is used as a negative electrode for LIBs, is not suitable for aqueous SIBs because sodium ions do not intercalate into graphite as well as lithium ions. Thomas P. et. al. studied graphite as a negative electrode and found that it exhibited only around 16 mAh/g capacity in $NaClO_4$/EC electrolyte solutions. [14] In aqueous electrolytes, using graphite becomes even more difficult due to hydrogen evolution, which renders the batteries unusable. [15]

1.3.1 Electrode materials for aqueous sodium ion batteries

One of the most important parts of the battery is the electrode active material. Active materials are the electrochemically active substances that directly participate in the chemical reactions (oxidation and reduction) to store and release energy. The main requirements for electrode active materials are: ability to accommodate sodium ions, good cyclability and stability, no reactions with the electrolyte solution or dissolution in the solvent, and,

ultimately, low cost, environmental friendliness, while possessing high ionic and, preferably, electric conductivity.[16] Many active materials for SIB electrodes, including layered metal oxides, Prussian blue analogues, carbon-based materials, polyanion compounds, and others, have been studied by researchers.[1] A perfect electrode would need to fulfil all the mentioned criteria, yet no such material exists, and the working-potential limitations of the HER and OER in the solvent further limit the number of materials that meet any of these criteria. [17]

Layered metal oxides (LMO) consist of alternating transition metal oxide polyhedra and Na^+ (or other cations) layers. These materials are usually simply synthesizable, have high capacities and energy densities.[18] LMOs are the most popular cathodes due to their widespread use in lithium-ion batteries. Yet they remain subject to several intrinsic degradation mechanisms, such as irreversible phase transitions, which can lead to capacity decay and oxygen loss during high-voltage operation, posing safety risks.[19]

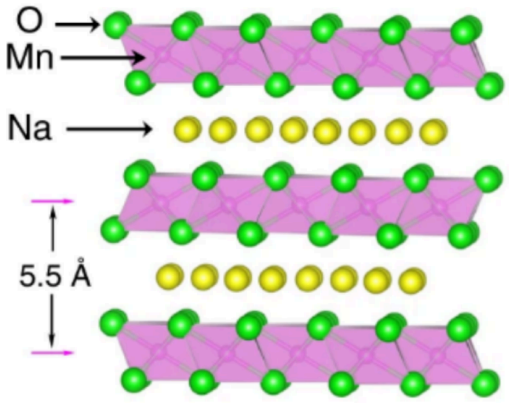

Figure 2. Structure of LMO ($Na_{0.67}MnO_2$). [20]

Prussian blue analogues (PBAs) (Fig. 3) can be used as both cathodes and anodes in sodium-ion batteries. PBAs are expressed as $A_xM_1M_2(CN)_6$. They are usually composed of an alkaline metal (A_x), transition metals (M_1, M_2) connected via CN^- ligands, resulting in a 3D network that is well suited to transport and accommodate sodium ions.[21]. PBAs show great stability and economic viability due to the use of inexpensive transition-metal precursors such as Fe, Mn, and Zn, and high theoretical capacities arising from two redox pairs. Yet these compounds pose several challenges. For example, these molecules contain coordinated water that prevents sodium intercalation, which results in a lower capacity. Also, the cube-like morphology and the large size of these crystals can slow sodium-ion intercalation, and as

such, they may need additional modifications such as porosity or increased vacancies in the crystal structure, which, while increasing intercalation speed, have shown more structural instability.[22]

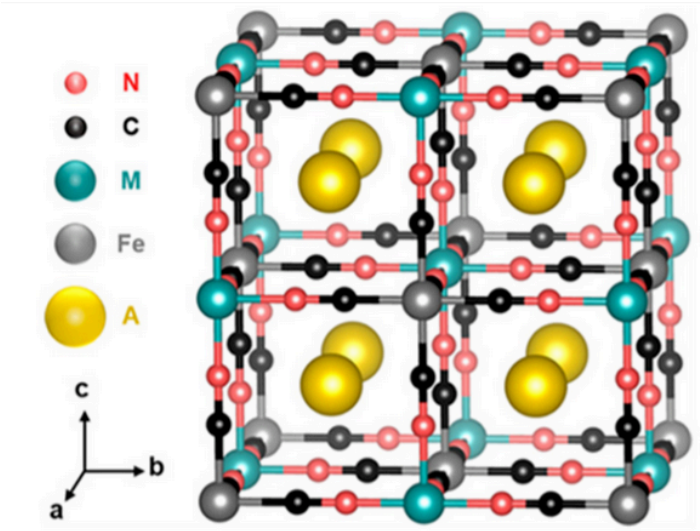

Figure 3: Crystal structure of PBA.[23]

Polyanion-type materials can be defined as compounds containing a series of $(XO)^{n-}$ tetrahedra, where X = P, S, Si, As, Mo, or W, strongly bonded with MO_x polyhedra where M represents a transition metal (Fig.4).[21,24] The open framework of these materials allows fast sodium ion conduction, and the covalent X-O bonds increase the stability and safety of the materials. Polyanion materials can be used as both positive and negative electrodes. However, they still have drawbacks: due to their high molecular weight, they exhibit relatively low capacity compared to PBAs and LMOs, as well as poor electrical conductivity.[21,24,25]

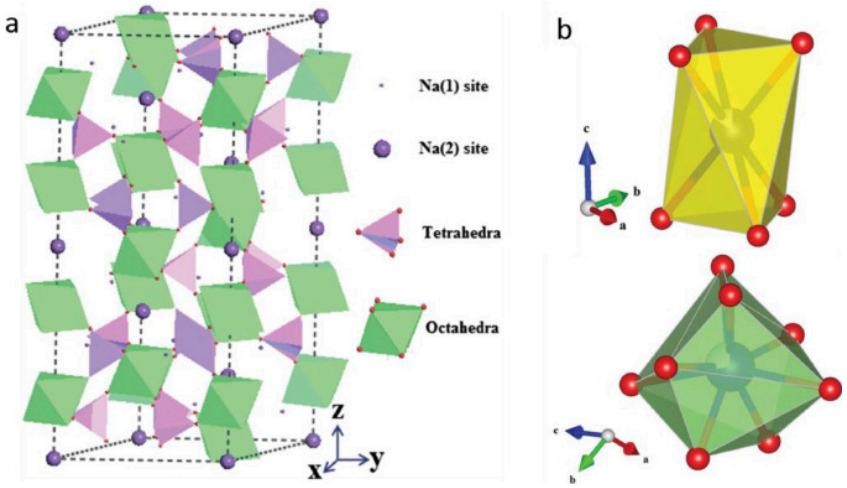

Figure 4. a) polyanion-type material crystal structure, b) polyhedral structures of Na_1 site and Na_2 site from the crystal structure[26]

Na super ionic conductors (NASICON) are a subgroup of polyanionic compounds that are usually described by a formula $Na_xM_2(PO_4)_3$, where M represents a transitional metal. These materials offer superior ionic conduction compared to other polyanionic materials, while remaining equally robust and stable.[27] Sodium titanium phosphate $NaTi_2(PO_4)_3$ (NTP) and Sodium Vanadium Titanium Phosphate (NVTP) emerge as leading electrode active materials in aqueous SIBs. NTP is an optimal negative electrode due to its low Ti^{4+} /Ti^{3+} redox couple potential of −0.60 V vs SHE and its high theoretical capacity of 132 mAh/g, which arises from its ability to intercalate 2 sodium ions reversibly.[28] Meanwhile, NVTP is the most favourable positive electrode due to its redox potential of 0.69 V vs SHE, which is assigned to the V^{3+} /V^{4+} redox couple, a rather high theoretical capacity of 124.8 mAh/g, and a coulombic efficiency of nearly 100% in both aqueous and organic solvents.[29,30] Both NTP and NVTP suffer from low electric conductivity, but these limitations can be resolved by reducing the particle size, doping or adding conductive additives.[31] After considering the properties of NVTP and NTP, they were selected as active materials for composite electrode synthesis in this work.

1.4 Binders for batteries

Binders play a crucial role in batteries by preserving the structural integrity of electrodes, i.e., acting as an adhesive between the electrode and the current collector, while also serving as a cohesive between the active material and carbon additives. Binders are typically used in small amounts because they do not participate in electrochemical reactions at the electrode; however, despite their small share of the overall electrode composition, binders have a significant impact on battery performance. To ensure reliable electrode performance, binder customisation is crucial.[32] Binders in batteries must be chemically, thermally, and electrochemically stable, cost-effective, and have good adhesion to the active material and current collector; they must also have good mechanical properties (elasticity and flexibility) and, finally, be sustainable. Good mechanical properties are needed for the electrode to withstand the forces of active material contraction and expansion during cycling. Electrochemical and chemical stability are vital to the battery's longevity. Thermal stability is important for the high-temperature curing process of the electrode as well as to prevent decomposition, volatilisation, or melting during battery operation. The cost-effectiveness and availability of binders are crucial considerations for large-scale battery manufacturing. While not necessary, it would be optimal for binders to exhibit good electronic conductivity, which would lead to fewer additives needed and ultimately yield energy-dense batteries.[32,33]

Poly(vinylidene) difluoride

The most commonly used binder is poly(vinylidene) difluoride (PVDF) (Fig. 5a) due to its chemical and electrochemical stability, and mechanical strength. Yet it does have its shortcomings. First of all, the poor adhesion to electrode components, especially with emerging high-capacity active materials, stems from its binding mechanisms, which primarily consist of van der Waals forces and mechanical interlocking. [34] PVDF is also an electrical insulator, meaning that electrodes need additional electrically conductive additives to function properly.[35] Also, PVDF's most common solvent is N-Methyl-2-pyrrolidone (NMP) - a toxic and rather expensive compound that has a high boiling point of 202 °C. The high boiling point results in more energy being wasted during solvent evaporation.[34,36] With this many drawbacks, a need for an alternative to PVDF arises, especially in aqueous

systems, which are known as the greener and more affordable alternative to conventional batteries.

Carboxymethyl cellulose

Carboxymethyl cellulose (CMC) (Fig. 5b) is derived from cellulose, commonly found in plants, making it an attractive green alternative to conventional battery binders such as PVDF. CMC exhibits good adhesion properties and porosity, which allows increased electrolyte penetration, and is compatible with many electrolyte solutions. [37] [38]However, it has relatively low mechanical strength, which can lead to degradation of the electrode under high stress conditions such as large volume changes or rapid charging rates. It also is not compatible with aqueous electrolyte solutions as they are water-soluable. Another consideration is the low thermal stability of CMC, which would limit the operational temperature range of CMC-based batteries.[38][38,39]

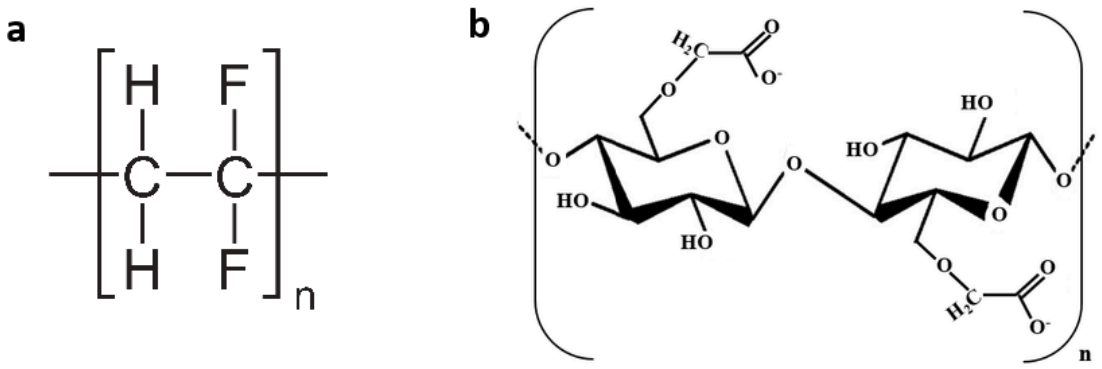

Figure 5: Structural formulas of a) PVDF and b) CMC

Polyvinyl alcohol

Polyvinyl alcohol (PVA) (Fig. 6B) is usually synthesised via hydrolysis of polyvinyl acetate (PVAc), which is not as green as CMC but much more environmentally friendly than the synthesis of PVDF. PVA also exhibits excellent adhesion to metallic surfaces due to its -OH groups. It also has great electrochemical stability and biodegradability, but it has its downsides. PVA is susceptible to chemical deterioration in highly acidic or basic environments. Also, the polymer is soluble in water, making it ineffective in aqueous batteries. [40]

Poly(vinyl butyral) (PVB)

Poly(vinyl butyral) (PVB) is an acetal which is formed by hydrolysing poly(vinyl acetate) and a further reaction with an aldehyde. The resulting product consists mostly of PVB and PVA fragments as well as a few acetyl segments that are randomly distributed throughout the polymer (Fig. 6) and can determine some of the polymer's properties.[41] The vinyl alcohol, as well as the few unreacted acetyl segments, primarily contribute to the polymer's adhesiveness due to their -OH and C=O groups, while butyral segments make it less susceptible to water in aqueous media, thereby increasing the polymer's stability. PVB is known as an excellent adhesive for many surfaces, although it is usually used as a glass interlayer.[42] In addition to its adhesive properties, PVB exhibits chemical and electrochemical stability, making it a potentially suitable binder for aqueous SIBs. Finally, PVB dissolves in inexpensive solvents such as 2-propanol, which is much more economically viable than NMP.[43]

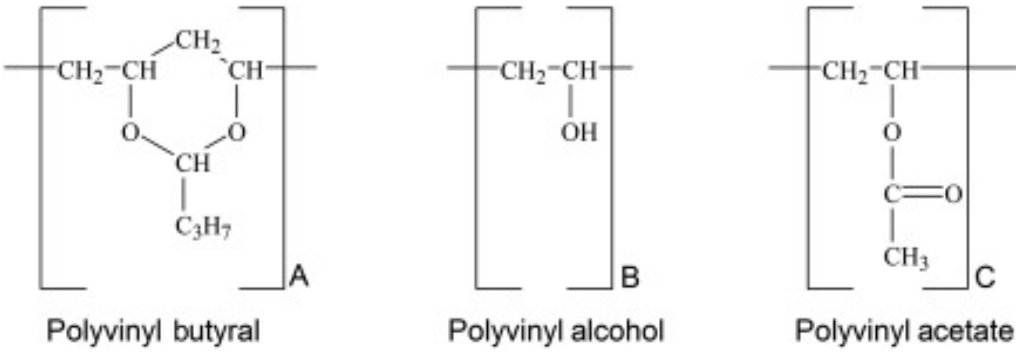

Figure 6. Structural formulas of PVB components: A) polyvinyl butyral, B) polyvinyl alcohol, C) polyvinyl acetate

Acrylic polymers

Acrylic polymers are considered a great alternative to PVDF, as they do not require toxic solvents and are considerably more budget-friendly than PVDF while exhibiting great adhesion to metals due to their carboxyl groups. The most studied compound in this group is polyacrylic acid, but because of its high water solubility, it cannot be used in aqueous batteries and, as such, will not be considered further.[36]

Poly(Isobutyl methacrylate) (PIBMA), poly(methyl methacrylate-ethyl acrylate) (PMMA-EA), and poly(methyl methacrylate-butyl acrylate) (MMA-BA) (Fig. 7) are potential binders for aqueous SIBs. These polymers exhibit strong adhesion to metals due to the carbonyl groups, are chemically and electrochemically stable, abundant, inexpensive, and easily soluble in inexpensive solvents like acetone. Another advantage of acrylic polymers is their adaptability as copolymers. By using monomers of different molecular mass, the mechanical properties of the copolymer can be changed, i.e., it can be made more flexible by using monomers with longer side chains. Additional MMA or EA chains increase the hardness, chemical stability, strength, and adhesion of the polymer, whereas longer chains, such as PIBMA or PBA, increase the polymer's flexibility while reducing adhesiveness.[44][45]

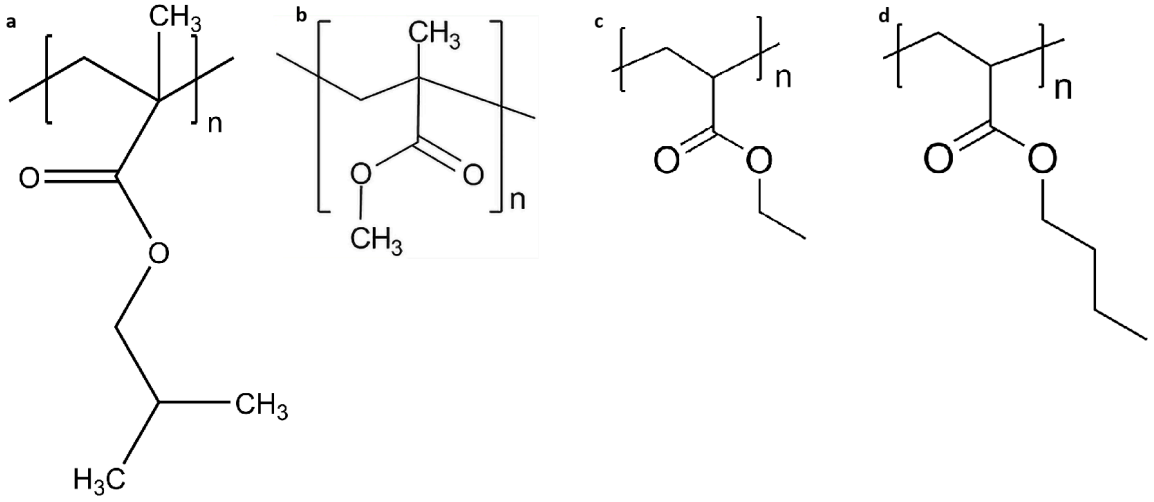

Figure 7. Structural formulas of a)PIBMA, b)PMMA, c) PEA, d)PBA.

Other polymers

Urea–isobutyraldehyde–formaldehyde (UIF) (Fig. 8) is a hydrocarbon resin that has the potential to be used as a binder for aqueous SIBs. UIF resins can be synthesised in two steps. In the first step, an a-ureido alkylation reaction occurs between urea and isobutyraldehyde to give, namely, 4-hydroxy-6-isopropyl-5,5-dimethyl-tetrahydro-pyrimidin-2-one (HIDTPO). Then HIDTPO reacts with formaldehyde and isobutyraldehyde to gradually produce the UIF resin.[46] The resulting product exhibits excellent adhesive properties due to the hydroxy and carbonyl groups, as well as chemical and thermal stability. It has both inexpensive precursors

and can be used with low-cost solvents such as 2-propanol. Although its electrochemical stability has not been studied extensively, it has potential as a binder for aqueous batteries.[47]

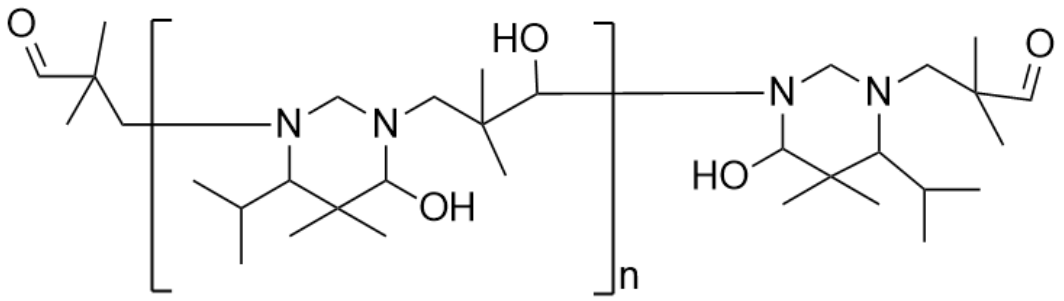

Figure 8. UIF Structure[47]

Ethylene vinyl acetate - styrene Isoprene Styrene (EVA-SIS) (Fig.9) resin could also be considered as a possible alternative to PVDF. EVA's main advantages include toughness, flexibility, good adhesiveness due to the carbonyl groups, and the ability to withstand low temperatures, yet it has a low softening point of 49-70 °C, depending on the ethylene-to-vinyl acetate ratio.[48] Meanwhile, styrene isoprene styrene increases the softening and melting point and adds extra elasticity to the copolymer.[49] Derived from petrochemical feedstocks, this material is inexpensive and can be dissolved in aliphatic and aromatic hydrocarbons, which are much more budget-friendly compared to NMP.

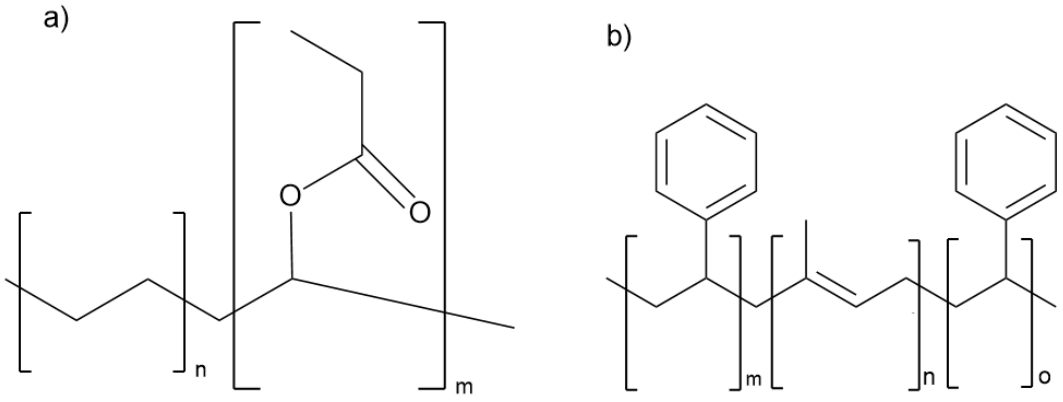

Figure 9 Structural formulas of a)EVA, b)SIS

For this study, the following polymers were chosen: PVB, UIF, EVA-SIS, and copolymers consisting of PIBMA, PMMA, PEA and PBA. The choice was made considering stability, price, adhesion to metal surfaces, and compatibility with aqueous electrolyte solutions. The named polymers will be analysed and compared with PVDF to determine whether they could outperform it and possibly replace it in aqueous SIBs.

2. EXPERIMENTAL

2.1 Materials

For the synthesis of active electrode materials the following materials were used: Sodium Carbonate (Na_2CO_3, 99.9% "Fisher scientific"), phosphoric acid (H_3PO_4, 6 mol/l "Chempur"), titanium isopropoxide ($Ti(OCH(CH_3)_2)_4$, 98+%, ÄCROS Organics"), tris(hydroxymethyl)aminomethane ($(HOCH_2)_3CNH_2$, 99+%, ÄCROS Organics"), hydrochloric acid (HCl, 35-38%, "Chempur"), 3-Hydroxytyramine hydrochloride ($(HO)_2C_6H_3CH_2CH_2NH_2 \cdot HCl$, 99%, ÄCROS Organics"), V_2O_5 (Chempur, 99%) vanadium(III)oxide (V_2O_3), which was prepared by heating V_2O_5 in N_2/H_2 (5% H_2) atmosphere, titanium dioxide (TiO_2, "Thermo scientific") and ammonium dihydrogen phosphate ($NH_4H_2PO_4$, pure, "Chempur"). For the electrode preperation the following materials were used: N-methyl-2-pyrrolidone (NMP, 99,5%, „Sigma Aldrich"), polyvinylidene fluoride (PVDF, HSV1800, „Kynar"), „Carbon Black", (CB, Super-P, „TIMCAL"), Paraloid B-44 (MMA-EA copolymer), Paraloid B-48N (MMA-BA copolymer), Paraloid B-67 (poly(Isobutyl methacrylate)), Paraloid B-72(ethyl methacrylate methyl acrylate copolymer), Polyvinyl butyral 30 (PVB), Laropal A81(Urea–isobutyraldehyde–formaldehyde resin), Regolite R1125 (ethylene-vinyl acetate - styrene Isoprene Styrene copolymer), Acetone ($(CH_3)_2CO$, pure, "Chempur"), 2-propanol (C_3H_8O, pure, "Chempur") and Hexane (C_6H_{14}, 99%, "Eurochemicals"). Apart from PVDF, all of the polymers were purchased from "Kremer Pigmente''.

2.2 Equipment/characterisation methods

Synthesised NTP and NVTP phase compositions were analysed by X-ray diffraction (XRD) using a Bruker D2 Phaser diffractometer with Cu Kα radiation. The measurements were made within the range of $5° < 2\theta < 70°$, with 0,01° scanning step.

Cyclic voltammetry (CV) was carried out by using Biologic SP-240 potentiostat-galvanostat at room temperature, utilising a 5 mV/s speed in a three-electrode

beaker-type cell. 1M Na_2SO_4 solution was used as the electrolyte, a Hg/Hg_2SO_4 electrode was used as a reference electrode and a graphite rod was used as a counter electrode. CV was recorded in -1.7 - +1.5 V vs Hg/Hg_2SO_4 voltage window.

Galvanostatic charge/discharge (GCD) cycling was carried out by using „GT-4008-5V10mA (Neware)“ battery tester in a three-electrode beaker-type cell, where the working and copper counter electrode were separated by a 1M $NaNO_3$ agarose salt bridge. The working electrode was placed in a 1M Na_2SO_4 solution, while the counter was in a 1M $CuSO_4$ solution. GDC cycling was performed at +0.5V- -0.5V and -1.35V - -1.0V vs Hg/Hg_2SO_4

2.3 Synthesis of active materials

$NaTi_2(PO_4)_3$ was synthesised via the conventional coprecipitation method. 14.560 g of concentrated H_3PO_4 was diluted with a small amount of deionised H_2O in order to reduce viscosity. 2.6248 g of Na_2CO_3 was added to the H_3PO_4 solution and left to react under stirring. Then, 28.230 g of $Ti(OCH(CH_3)_2)_4$ was added to isopropanol in order to prevent contact with oxygen, followed by an immediate addition to the H_3PO_4 and Na_2CO_3 containing beaker. The resulting mixture was left to react under stirring for 30 min. The 2-propanol and H_2O were then evaporated utilising a hotplate, and the resulting powder was ground and calcined in a muffle furnace at 700 ^oC for 8h under an air atmosphere. The acquired particles were reground and ball-milled in isopropanol at 350 rpm for 1h and dried at 80 ^oC.

$Na_2VTi(PO_4)_3$ was synthesised via solid-state reaction. 0.9866g of Na_2CO_3 were mixed with 0.6976g of V_2O_3, 0.7463g of TiO_2 and 3.2121g of $NH_4H_2PO_4$ by ball-milling in isopropanol at 350 rpm for 1h. The resulting mixture was dried at 80 ^oC and calcined under N_2 at 350 ^oC, re-ground and calcined again under N_2 at 800 ^oC for 12 h. The resulting particles were ball-milled in isopropanol at 350 rpm for 1h and dried at 80 ^oC.

Both NVTP and NTP particles were coated with carbon according to the following procedure: The synthesised particles were dispersed in 0.3 mol/l tris(hydroxymethyl)aminomethane-HCl (tris-HCl) buffer, in a separate beaker, and dopamine-HCl was dissolved in tris-HCl buffer. The mass ratio of tris-HCl to active material was 3:200, and the mass ratio of dopamine-HCl to active material particles was 3:5. The dopamine-HCl solution was added to the particle dispersion and stirred for 16h. The resulting

particles were centrifuged at 7000 rpm and washed with deionised water four times. The washed particles were dried at 80 ^{o}C and pyrolysed under N_2 at 700 ^{o}C for 2h, ball-milled in isopropanol at 350 rpm for 1h, and dried at 80 ^{o}C.

2.4 Electrode preparation

The electrodes were prepared by mixing the active material (NVTP or NTP) with Carbon black (CB) and a binder (PVDF, Paraloid B-44 (PB44), Paraloid B-48 (PB48), Paraloid B-67 (PB67), Paraloid B-72), Poly vinyl butyral 30 (PVB), Laropal A81(LA81), Plexigum PQ611 (PGPQ) or Regolite R1125 (RR1125)), respectively, in a mass ratio of 7:2:1. The active material and CB were dried in a vacuum oven (5 mb, 120 ^{o}C, 2 h). The dry components were then homogenised in a high-energy ball mill (Retsch PM400) with 3 mm diameter zirconium oxide balls at a speed of 150 rpm. The resulting mixture was then separated from the balls, and a binder and a solvent were added. The mixture was returned to the mill with 5 mm diameter balls and homogenised for 2 h at a speed of 350 rpm. After homogenization, casting the slurry as a 300 μm thick wet film on the aluminium foil followed. In order to remove the solvent, the electrodes were dried in a fume hood overnight, except for the electrode containing PVDF. Electrodes with a diameter of 13 mm were punched out from the resulting coatings and then transferred to a 15 mm diameter stainless steel mesh (316L, #325, Inoxia Ltd) using a hydraulic press (7 tons). After transfer, the aluminium foil is removed. Transfer of the electrode is necessary due to the corrosion of aluminium in both acidic and alkaline media, which is observed at the electrode surface during charging or discharging.

3. RESULTS AND DISCUSSION

3.1 Structure and purity of active electrode materials

In order to determine the structure and phase purity of the synthesised active materials, XRD analysis was carried out for both $NaTi_2(PO_4)_3$ (NTP) and $Na_2VTi(PO_4)_3$ (NVTP), and is shown in Fig. 1. In both materials, the observed sharp peaks indicate a high degree of crystallinity. The recorded patterns identified the NASICON-type structure with $R\bar{3}c$ (No. 167) space group and agree very well with those reported in the literature.[50]

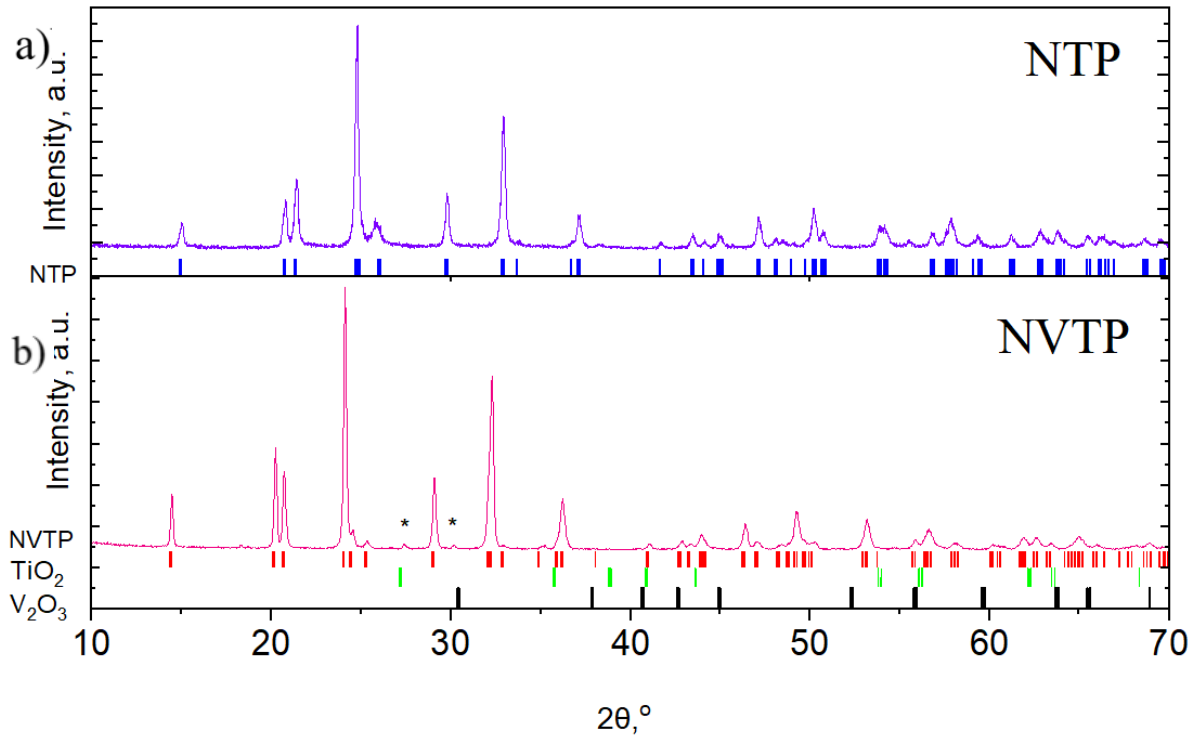

*Figure 10. X-ray diffraction patterns of synthesised a) NVTP and b) NTP powders with the unreacted material marked by *.*

From the NTP diffraction pattern (Fig. 1 a), it is apparent that the phase is pure without any unreacted material, whereas in the NVTP (Fig. 1 b) case, a few small additional peaks can be noticed due to unreacted material. This difference is apparent due to the different synthesis methods of these materials; solid-state synthesis is known to produce some

unreacted products due to insufficient homogeneity and slow diffusion. Due to slow diffusion, precursors are prevented from travelling through the material efficiently; as such, the resulting material contains a small amount of unreacted TiO_2 and V_2O_3, whereas the co-precipitation method does not face these problems and produces a much purer product.

3.2 Adhesion studies on polymers and their composites

To determine the adhesion properties of the selected polymers and composites, a preliminary adhesion study was conducted both with and without any solid additives. Polymer solutions were cast on a steel foil, and discs were punched out. The polymer-coated steel foil discs were placed in neutral pH 1M Na_2SO_4 and pH 4 Na_2SO_4 - boric acid buffer solutions for seven days with daily agitation. The acidic pH was chosen to observe the polymers, which form hydrogen bonds due to hydroxy groups and tend to oxidise at acidic pH. After a week, the samples that had not fallen apart were lightly scratched with tweezers to test the polymers' adhesive properties. The results of this study are presented in Table 1.

Binder	Anode in pH 4 Buffer solution	Anode in Na_2SO_4 solution	Polymer in pH 4 Buffer solution	Polymer in Na_2SO_4 solution
LA81	Detached after 24 h	Detached after 24 h	Detached after 24 h	Detached after 24 h
RR1125	Fell apart in 24 h	Fell apart in 24 h	Fell apart in 24 h	Fell apart in 24 h
PGPQ	Was removed by mechanical agitation after a week	Was removed by mechanical agitation after a week	Stayed on the surface	Was removed by mechanical agitation after a week
PB67	Was removed by scratching after a week	Was removed by mechanical agitation after a week	Was removed by scratching after a week	Was removed by mechanical agitation after a week
PB72	Detached after 24 h	Was removed by mechanical agitation after a week	Was removed by scratching after a week	Was removed by mechanical agitation after a week
PB82	Detached after 48 h	Was removed by mechanical agitation after a week	Detached after 48 h	Was removed by mechanical agitation after a week
PB48N	Detached after 24 h	Was removed by mechanical agitation after a week	Partially stayed	Detached after 48 h
PB44	Detached after 24 h	Was removed by mechanical agitation after a week	Detached after 48 h	Detached after 48 h
PVB	Was removed by mechanical agitation after a week	Was removed by mechanical agitation after a week	Stayed on the surface	Was removed by mechanical agitation after a week
PVDF	Detached after 24 h	Detached after 48 h	Detached after 48 h	Detached after 48 h

Table 1. The observed period of time between polymer and electrode-coated disc submersion in 1M Na_2SO_4 and pH 4 1M Na_2SO_4 solutions and their detachment from the disc's surface.

This study showed that EVA-SIS-based RR1125 is not stable in both acidic and neutral electrolyte solutions and disintegrates within 24 hours. Similar tendencies were observed in cast electrodes that were not submerged, as they exhibited extensive cracking and fell apart when a thicker layer of electrode slurry was applied or if the foil was bent. UIF-based LA81 performed better, as it did not fall apart but did get dislodged from the metal surface within 24 hours, both as a single polymer and a cast electrode. PVDF performed better, as its electrode in neutral electrolyte and pure cast polymer remained on the surface after being agitated the first time after 24h, with the exception of the cast electrode in the buffer solution, yet the rest of them still dislodged after 48h. The acrylic polymers showed various results, depending on their side chain length. Of the acrylic polymers, PB-44 (based on MMA-EA) performed the worst and, in most cases, got dislodged from the metal surfaces within 48h. PB-48N (MMA-BA), PB-72(EM-MA) and PB-82 performed similarly, and although they performed well in neutral pH, an acidic environment made their electrodes dislodge from the surface within 48h. Although based on the same copolymer, P8-82 (MMA-EA) performed better than PB-44, which can be attributed to different amounts of polymers in the copolymers, in turn making PB-44 harder and more brittle. PGPQ (IBMA), PVB and PB67 (IBMA) were the best performing polymers as they remained on the metal surfaces after a week of daily agitation. After the week, the electrode and polymer surfaces were scratched, and PVB and PGPQ cast polymers were the only ones that did not dislodge or fall apart while mechanical agitation was applied.

3.3 Electrochemical studies of polymers and polymer containing electrodes

To assess the electrochemical stability of the polymers and determine whether they are suitable as electrode binders in aqueous systems, cyclic voltammetry was performed on electrodes composed of 40% CB and 60% polymer. The results are shown in the annex. The minor peaks observed in the voltammograms were attributed to plasticisers, initiators, and other additives that react during the first few cycles and exhibit no significant electrochemical activity in subsequent cycles. To confirm this, cyclic voltammetry was performed with NTP-containing electrodes, as shown in the annex. These voltammograms also showed no significant electrochemical activity beyond the oxidation of Ti atoms at -1.0V vs Hg/Hg_2SO_4 and following reduction of the mentioned Ti at -1.35 V, thus further confirming the stability of the mentioned polymers.

Further electrochemical evaluation of selected polymers was conducted via galvanostatic charge-discharge cycling of the NTP-based composite electrodes in order to determine the electrode's capacity and cycling stability compared to a PVDF-NTP-based electrode, and is displayed in Fig. 11-12. The tested composites showed promising results: most of the acrylic polymer-containing electrodes exhibited results comparable to the PVDF-containing one. High initial capacities of 87 mAh/g, 102 mAh/g, 86 mAh/g, and 81 mAh/g, attributed to PB67, PB48N, PB82, and PB44-containing composites (Fig.11), similar to PVDF-based one, accounting for 90 mAh/g. Yet their capacity retentions were lower: 53.59% for PB67, 37.42% for PB48N, 50.88% for PB82, and 41.07% for PB44 containing electrodes, compared to 67.97% for PVDF containing one. The below-average performance of PB44 can be attributed to its short side chains, which make the polymer less malleable and more brittle, making it hard to work with and perform worse during the galvanostatic cycling as the material is not flexible enough to resist cracking during the expansion and retraction of the active material.

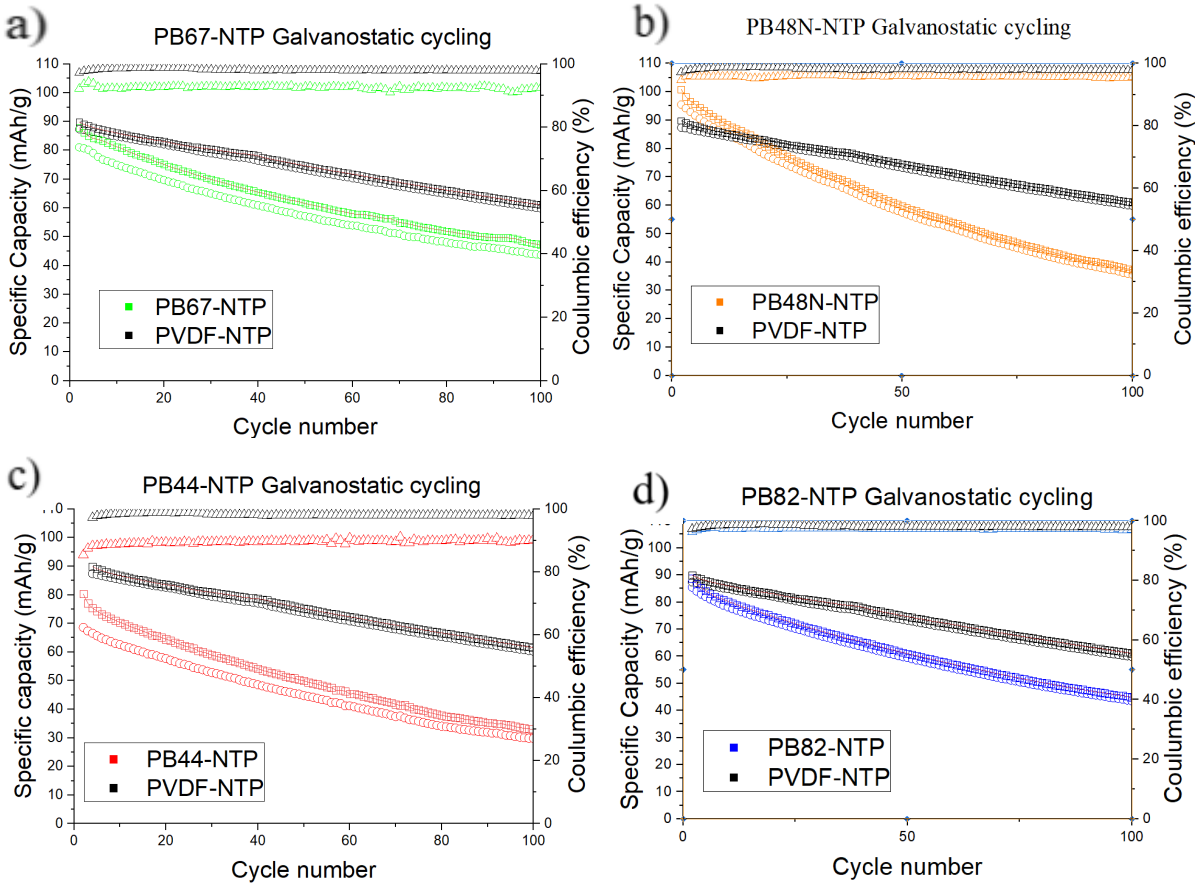

Figure 11. Galvanostatic charge- discharge cycling of a) NTP-PB67, b) NTP-PB48N, c) NTP-PB44, d) NTP-PB82 based electrodes with comparison to NTP-PVDF.

PVB and PGPQ-based composites exhibited a high initial capacity of 105 mAh/g and 101 mAh/g, respectively, which was greater than the PVDF-based one, although the capacity fade for the PVB-based composite was greater, and after 100 cycles, it was reduced to only 44.5 mAh/g (41.21%) compared to PVDF-based 63 mAh/g (67.97%), while the PGPQ-based composite retained a 52.7 mAh/g (52.18%) capacity (Fig. 12 a, b). The only underperforming polymers were RR1125 and LA81, which exhibited initial capacities of only 52 mAh/g and 71 mAh/g and a capacity retention of 62.58% and 39.59%, respectively(Fig.12 c, d). As all the used polymers are electrochemically stable as indicated by the CV data within -1,7 to +1,5 V vs $Hg/HgSO_4$, the different performance of these electrodes is attributed to their chemical properties. During the adhesion studies, it was noted that most of the chosen polymers performed worse at lower pH values, and as the electrode is being charged and

discharged, the local pH level fluctuates, which has a detrimental effect on some of the binders.[51] This effect can be clearly seen in EVA (present in RR1125) or urea formaldehyde resins (the main component of LA81) that have functional groups used for chemical binding.[52], [53]

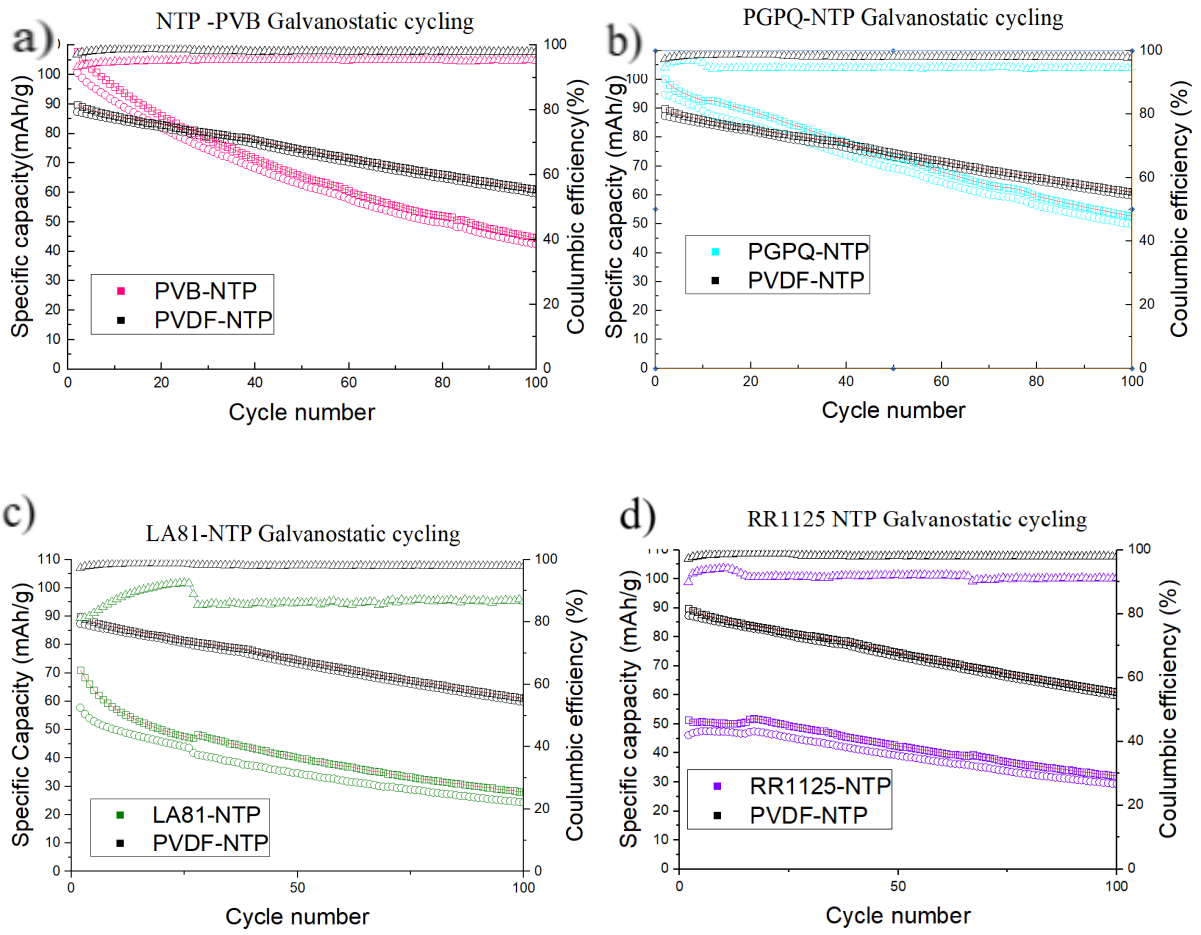

Figure 12. Galvanostatic charge- discharge cycling of a) NTP-PVB, b) NTP-PGPQ, c) NTP-LA81, d) NTP-RR1125 based electrodes, with comparison to NTP-PVDF

After the data were analysed, it was concluded that the optimal binders for composites, in terms of electrochemical stability, adhesion, and capacity, were prepared using PVB, PGPQ, and PB67. Composites made with these polymers were further electrochemically studied via galvanostatic cycling in sealed beaker cells under N_2 bubbling to mitigate degradation of the active material caused by O_2 present in the electrolyte solution and to assess the long-term stability of the composite materials.[54] The results are presented in Fig.13. Under N_2 bubbling, a significant improvement of electrochemical parameters was noticed, although initial capacities remained similar (106 mAh/g for PVB, 108 mAh/g for PGPQ and 86 mAh/g

for PB67 containing composites) the capacity retention was increased greatly (43.53% for PB67 16.01% for PVB and 56.8% for PGPQ after 300 cycles). These results were compared to the PVDF-based composites' behaviour, which had an initial capacity of 105 mAh/g and retained 31.34% of its initial capacity, and it was obvious that both the PVB and PB67-based composites had similar results to the PVDF. Although PVB had a larger initial capacity, it also exhibited greater capacity fade, while PB67 exhibited lower initial capacity and lesser fade compared to the PVDF-based one. The PGPQ-based composite outperformed them with its highest initial capacity, lowest capacity fade and superior adhesion in aqueous electrolyte solutions. Although the PGPQ and PB67 are both based on the IBMA polymer, their performance differences can be attributed to variations in additives, polymerisation degree or simply due to small differences during the electrode preparation.

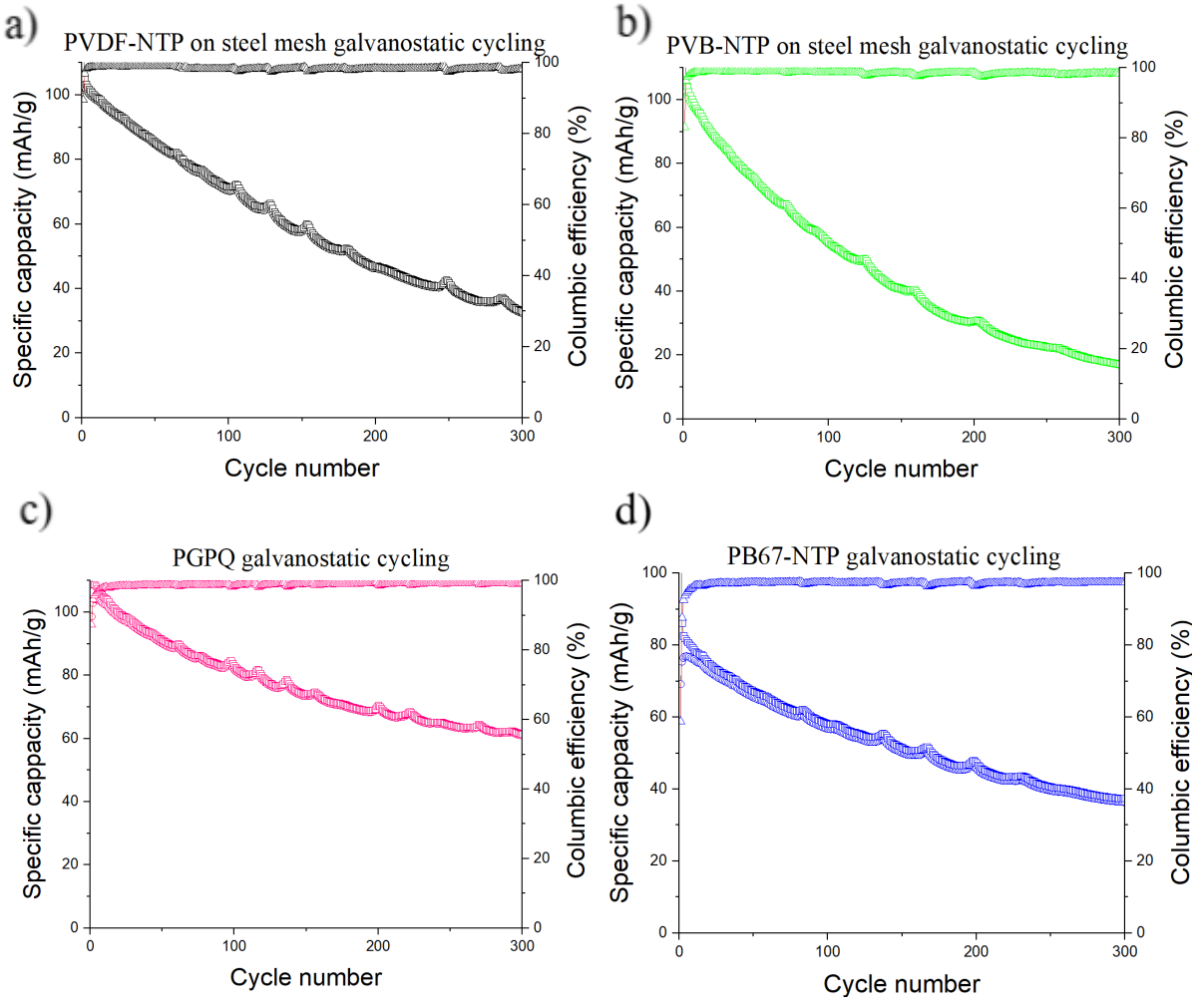

Figure 13. Galvanostatic cycling of a) NTP-PVDF, b) NTP-PVB, c) NTP-PGPQ, d) NTP-PB67 under N_2 bubbling.

To further investigate the adhesiveness of the chosen composite electrode, electrodes were cast onto stainless steel foil and galvanostatically cycled. Metal foil is the more common current collector for batteries, as it is lighter and requires fewer steps and, in turn, less time. Hence, when producing electrodes, it would be optimal for a polymer to exhibit strong adhesion to the steel foil to be applicable in batteries. The GCD cycling on stainless steel foil results are presented in Fig. 14. Due to their poor adhesiveness in aqueous media, PVDF composites were not included in this study, and the PB67-based composite detached from the steel foil surface after a few cycles and, as such, was not studied further Fig. 14.

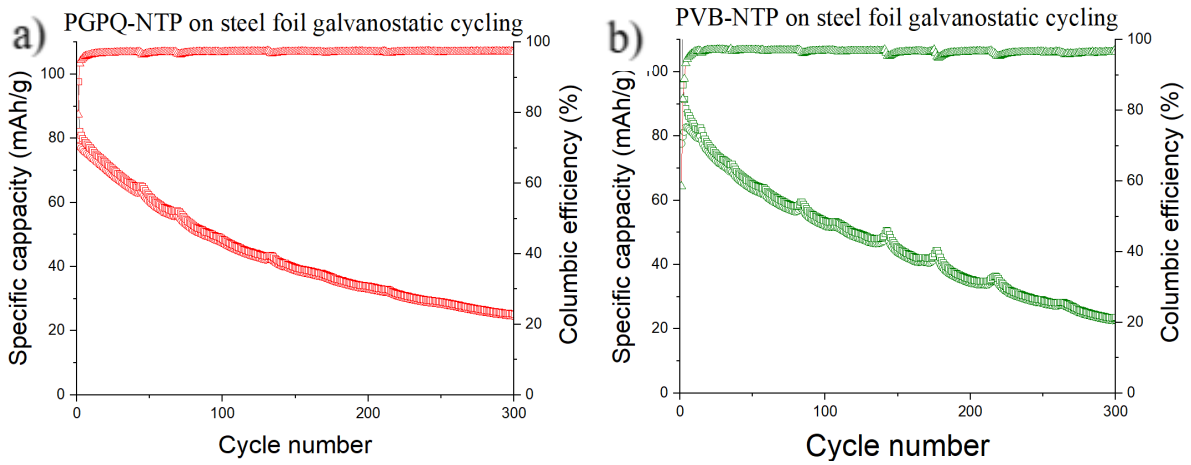

Fig.14 galvanostatic cycling of a) NTP-PGPQ, b) NTP-PVB cast on steel foil, measured under N_2 bubbling.

The remaining composites performed worse on steel foil compared to steel mesh, and as they exhibited lower initial capacities, 96 mAh/g for PVB and 82 mAh/g for PGPQ and a relatively low capacity retention of 24.63% for PVB and 30.84% for PGPQ after 300 cycles. These differences mainly arise due to the difference between binding in steel foil and mesh. In the case of steel mesh, the composite is simply pressed onto the surface of the current collector, and the primary polymer property governing the electrode's performance is cohesion. Meanwhile, in the stainless steel foil case, polymers must exhibit good adhesion to the current collector. As such, the lower initial capacity is caused by the production processes. During the punching out of the electrodes, the largest amount of force is exerted at

the edge of the electrodes. Also, in the beaker cell, the edges of the electrodes are further pressed against, which results in some breakage of the electrode at its edge fig. 15.

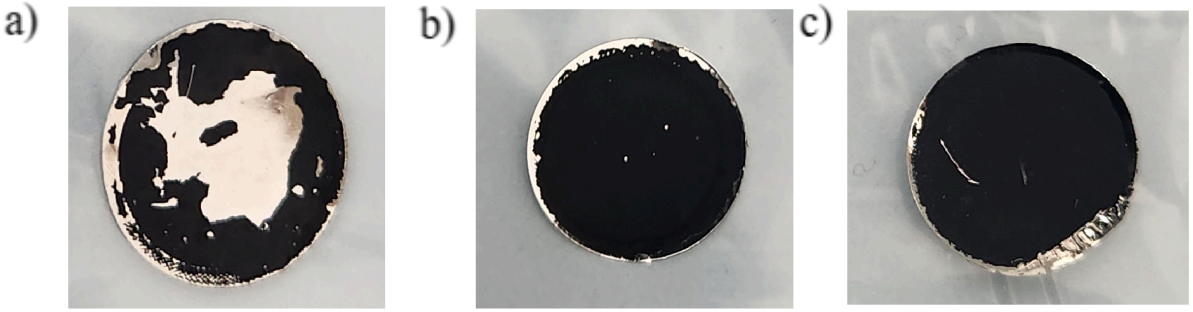

Figure 15. Images of a) NTP-PB67, b) NTP-PVB, and c) NTP-PGPQ-based composites after galvanostatic cycling.

To further explore the chosen polymer's behaviour in positive electrodes, galvanostatic cycling was performed on NVTP-based composites both pressed onto steel mesh and cast on steel foil. The results are shown in Fig.16. Although all materials showed low initial capacities, this was expected, as only the $V^{3+} \leftrightarrow V^{4+}$ redox couple was exploited; accordingly, only half of the theoretical capacity of 124.8 mAh/g could be utilised. The initial capacities for composites pressed onto steel mesh were around 40 mAh/g, and due to NVTP's exceptional stability, after 100 cycles, it remained similar. In the case of electrodes cast on steel foil, similarly to the negative electrodes, PVDF and PB67-based electrodes did not retain their integrity, and the majority of the material floated away from the current collector surface. The PVB and PGPQ-based composites, just as in the case of negative electrodes, exhibited lower initial capacities than their mesh-pressed counterparts, but overall showed similar capacity retention except for the NVTP-PVB-based electrode, where, around the 74th cycle, the capacity sharply decreased. This was attributed to a part of the electrode dislodging from the foil's surface and entering the electrolyte solution.

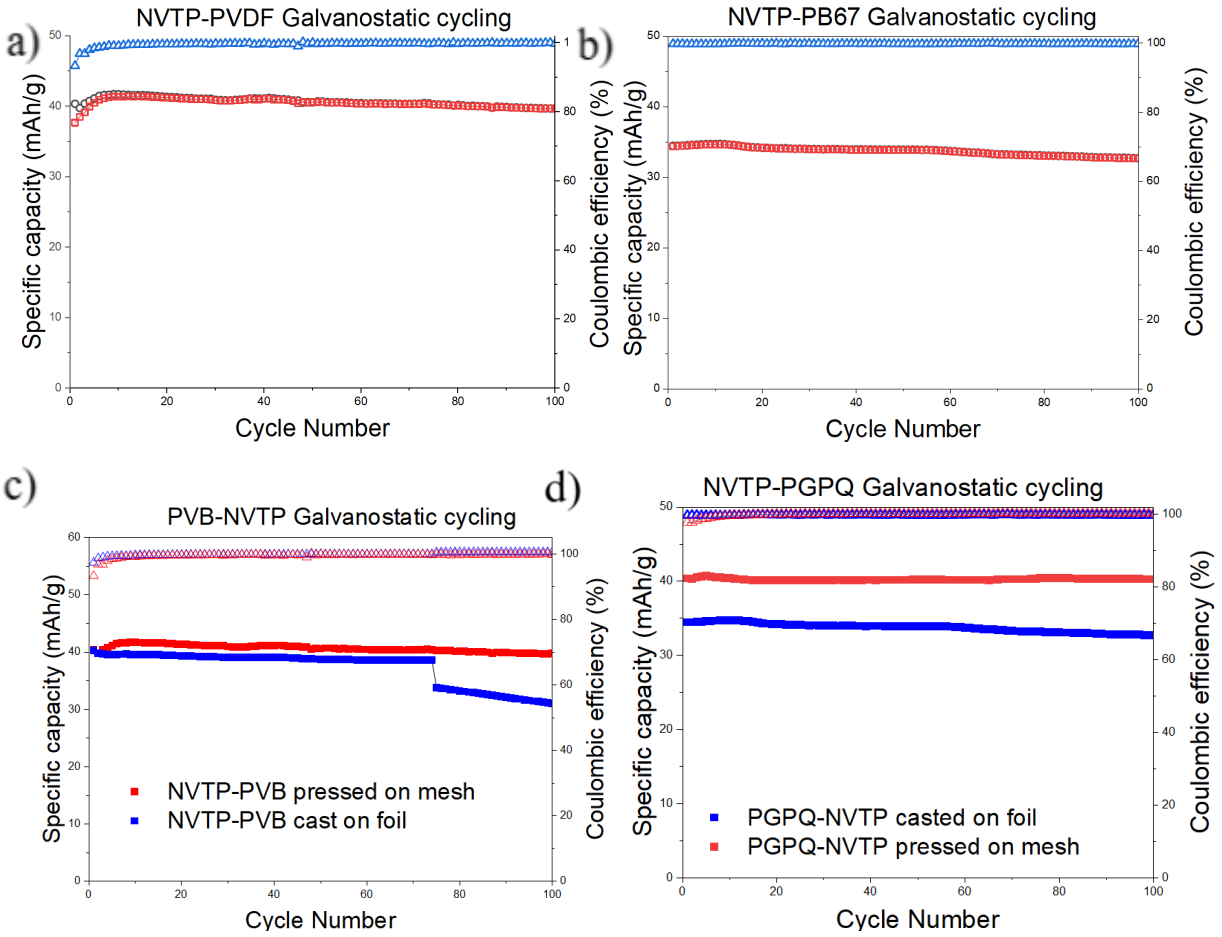

Figure 16. Galvanic cycling of electrodes based on a) NVTP-PVDF on steel mesh, b) NVTP-PB67 on steel mesh, c) NVTP-PVB on steel mesh, d) NVTP-PVB on steel foil, e) NVTP-PGPQ on steel mesh, f) NVTP-PGPQ on steel foil.

3.4 Study of electrode surface morphology

To understand the partial or total degradation of the electrodes better, SEM images of the electrode surfaces were taken before and after galvanostatic cycling. The results are shown in Fig. 17-19. Due to their inability to maintain their form and adhesiveness in water, PVDF-based electrodes pressed onto stainless steel mesh are presented (Fig.17); even in this case, surface cracking is clearly visible. These cracks usually appear due to stress and strain during cycling or drying. As the pre-cycled material contains little to no cracks and the electrolyte evaporation was carried out at room temperature, cracking during cycling remains

the most likely explanation. Surface cracking can lead to significant loss of performance; therefore, an optimal electrode should not exhibit such surface defects.[55]

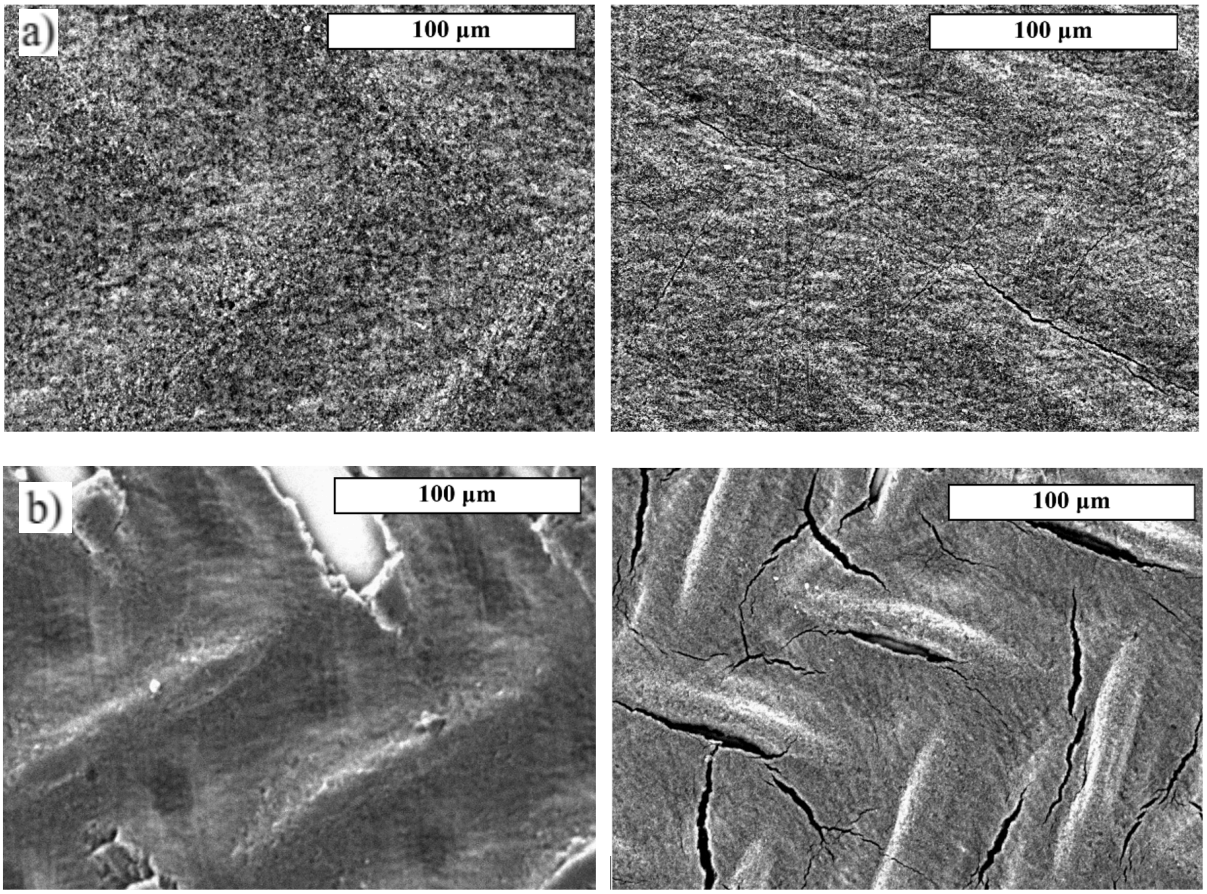

Figure 17. SEM images of a) PVDF-NTP on mesh, b) PVDF-NVTP on mesh, pre galvanic cycling (on the left) and post galvanic cycling (on the right).

Fewer surface cracks can also be noticed on the surface of PVB-NTP and PVB- NVTP electrodes compared to PVDF-based ones (Fig.18). Cracks, although fewer, can be noticed in the PVB-NTP electrodes before cycling, and larger crevices can be noticed after. In PVB-NVTP, surface deformities can be noticed pre- and post-cycling, and just as cracking beforehand can be attributed to the preparation process, as cracking and deformations can occur during the evaporation of the solvent.

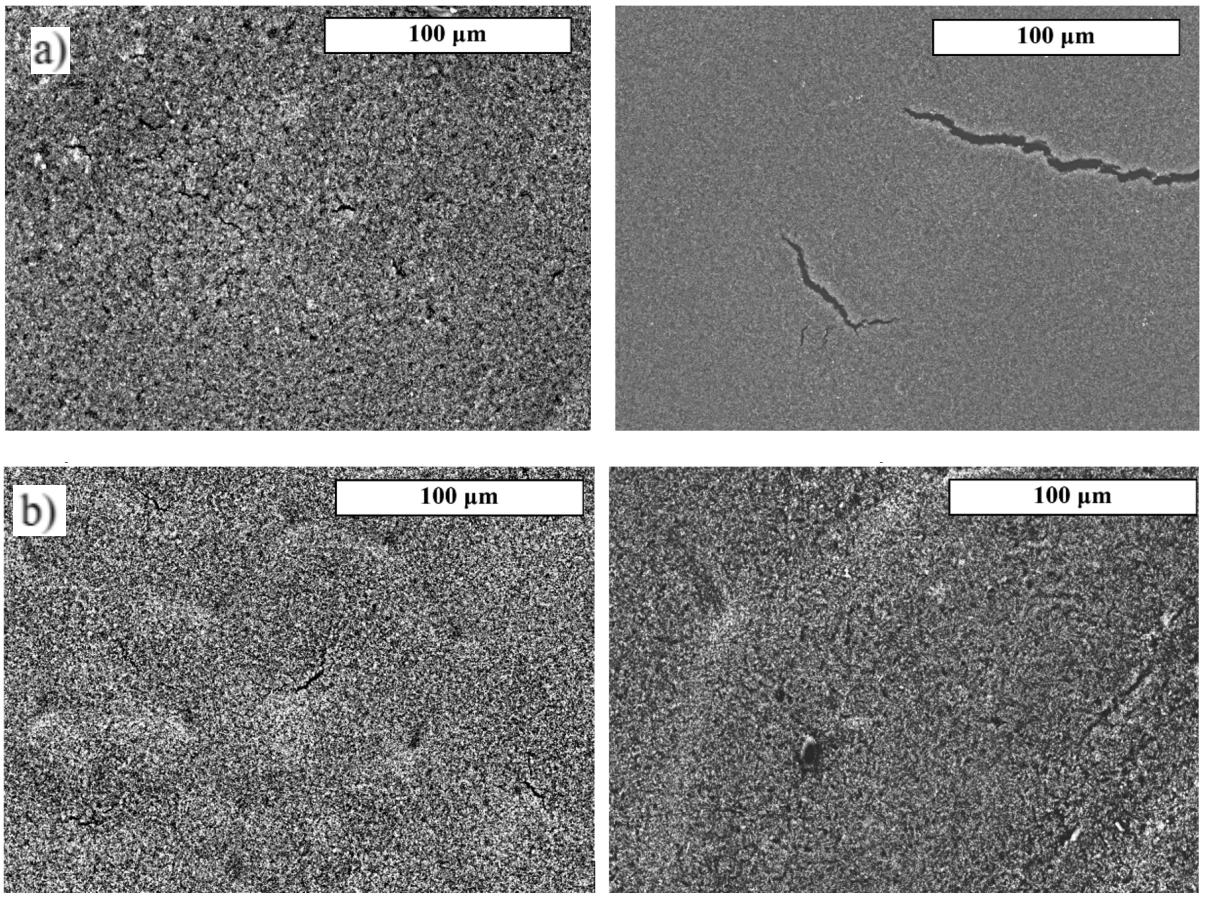

Figure 18. SEM images of PVB-NTP on foil, d) PVB-NVTP on foil, e)PGPQ-NTP on foilpre galvanic cycling (on the left) and post galvanic cycling (on the right).

The fewest cracks were seen on PGPQ-based electrodes (Fig.19). This was quite surprising, as PGPQ was dissolved in acetone, and having the most volatile solvent, it was expected that PGPQ-based electrodes would exhibit the most cracking. The crack-free surface explains the greater capacity retention of PGPQ-based electrodes.

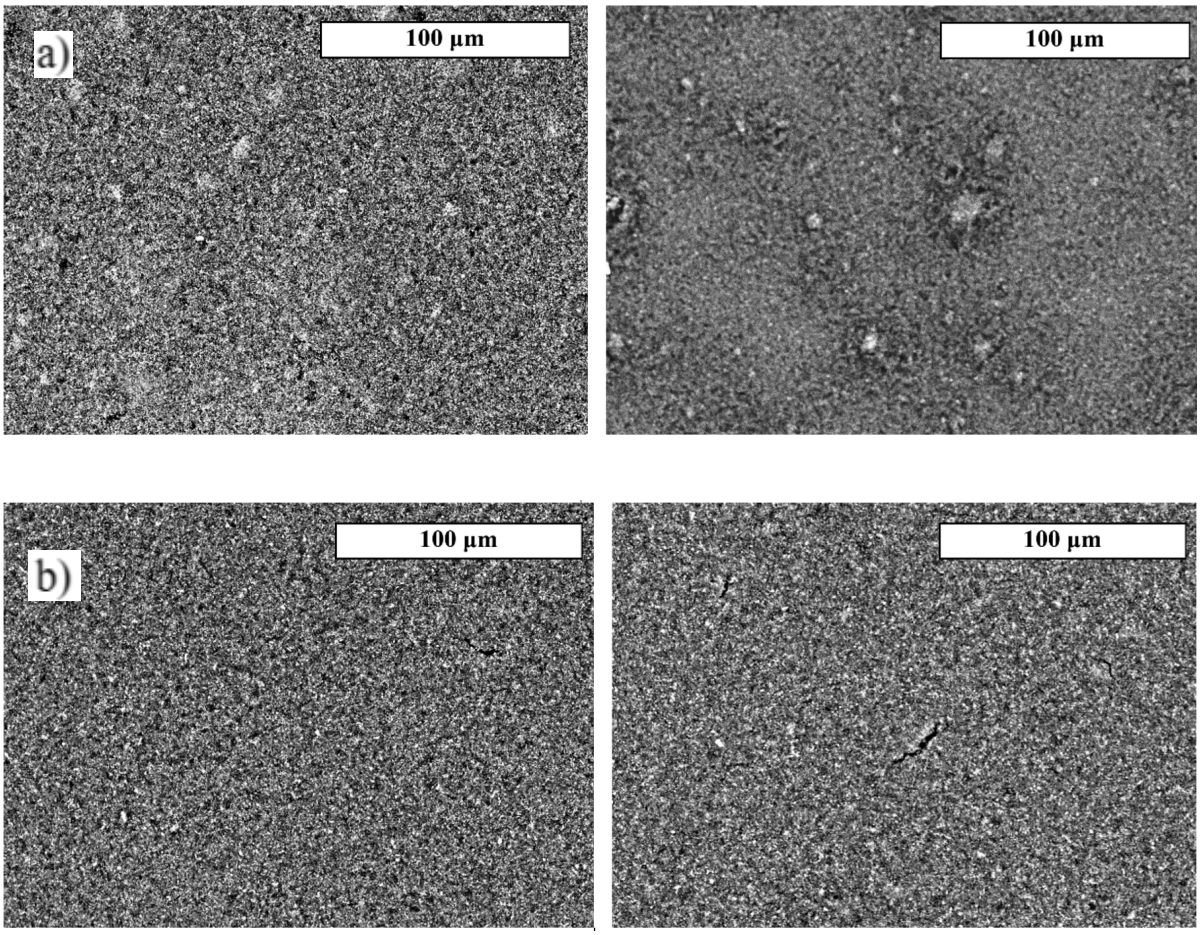

Figure 19. SEM images of e)PGPQ-NTP on foil, f) PGPQ-NVTP on foil, electrodes pre galvanic cycling (on the left) and post galvanic cycling (on the right).

The images of the PVB, PGPQ, and PB67 electrodes pressed onto steel mesh (Annex 2) show no particular difference pre- and post-cycling, and the main differences observed among these electrodes are in the amount of material pressed into the mesh. These differences arise due to the different behaviour of these materials during the casting and drying processes. PVB-based electrodes were the easiest to work with, as the electrode slurry had a viscosity comparable to the PVDF-based slurries; it did not crack or dislodge from the foil's surface during drying and was overall easy to handle. PB67 exhibited the most cracking, especially in thicker layers, which would ultimately completely fall apart during the drying process. PGPQ-based electrodes showed some cracking in the thicker layers and could never reach the thickness of PVB-based electrodes, but were not as difficult to handle as the PGPQ ones.

CONCLUSIONS

1) The preliminary adhesion study demonstrated significant differences in the stability and adhesion performance of the investigated polymers and composites: EVA-SIS-based RR1125 and UIF-based LA81 exhibited poor adhesion; acrylic PB-44, PB-48N, PB-72, and PB-82 showed better but still limited adhesion; and PVB, PGPQ, and PB67 were superior.
2) Cyclic voltammetry proved that the polymers were not electrochemically active within -1.7 to +1.5 V vs $Hg/HgSO_4$ range and could be further explored by GCD cycling. GCD cycling of positive and negative electrodes pressed on steel mesh helped to choose PGPQ, PVB and PB67 as the best performing electrodes, which were further tested via GCD cycling of positive and negative electrodes casted on steel foil, showed that PVDF and PB67 based electrodes dislodged from the surface during cycling, while PGPQ and PVB based electrodes stayed on the surface, although a small piece of PVB enegative electrode did get dislodged.
3) During the electrode surface study, defects on the electrode surface were observed. PVDF-based mesh pressed electrodes exhibited the most cracking pre and post-GCD cycling, PVB-based electrodes exhibited some cracking and nonuniformity, and PGPQ-based electrodes showed little to no cracks and were quite uniform.
4) Considering the results of these experiments, PGPQ was chosen as the most advantageous polymer due to its excellent electrochemical and adhesive properties, with PVB as another plausible alternative due to its good adhesiveness and ease of handling.

LITERATURE

1. Zhao G, Gaddam RR. Handbook of Sodium-Ion Batteries: Materials and Characterization. CRC Press; 2023.

2. Linden D, Reddy T. Handbook of Batteries. McGraw-Hill Professional; 2002.

3. Besenhard JO, Daniel C. Handbook of Battery Materials. 2012.

4. Anti-aging for batteries? – secrets of science. [cited 20 Apr 2026]. Available: https://www.shimadzu-webapp.eu/magazine/issue-2016-2_en/anti-aging-for-batteries/

5. Zhang J, Zhang L, Liu H, Sun A, Liu R-S. Electrochemical Technologies for Energy Storage and Conversion. John Wiley & Sons; 2012.

6. Zhou G. Design, Fabrication and Electrochemical Performance of Nanostructured Carbon Based Materials for High-Energy Lithium–Sulfur Batteries: Next-Generation High Performance Lithium–Sulfur Batteries. Springer; 2017.

7. Menictas C, Skyllas-Kazacos M, Lim TM. Advances in Batteries for Medium and Large-Scale Energy Storage: Types and Applications. Elsevier; 2014.

8. Kumta PN, Hepp AF, Datta MK, Velikokhatnyi OI. Lithium-Sulfur Batteries: Advances in High-Energy Density Batteries. Elsevier; 2022.

9. Thermal hazard comparison and assessment of Li-ion battery and Na-ion battery. Journal of Energy Chemistry. 2025;102: 18–26.

10. Inamuddin, Boddula R, Ahamed MI, Asiri AM. Sodium-Ion Batteries: Materials and Applications. Materials Research Forum LLC; 2020.

11. Tapia-Ruiz N, Armstrong AR, Alptekin H, Amores MA, Au H, Barker J, et al. 2021 roadmap for sodium-ion batteries. J Phys Energy. 2021;3: 031503.

12. Ponrouch A, Marchante E, Courty M, Tarascon J-M, Rosa Palacín M. In search of an optimized electrolyte for Na-ion batteries. Energy Environ Sci. 2012;5: 8572–8583.

13. Sawicki M, Shaw LL. Advances and challenges of sodium ion batteries as post lithium ion batteries. RSC Adv. 2015;5: 53129–53154.

14. Electrochemical insertion of sodium into hard carbons. Electrochimica Acta. 2002;47: 3303–3307.

15. Alcorn FM, Kuntz KL, Druffel DL, Warren SC. Aqueous Intercalation of Graphite at a Near-Neutral pH. ACS Applied Energy Materials. 2018 [cited 27 Feb 2026]. doi:10.1021/acsaem.8b01101

16. Wu Y. Lithium-Ion Batteries: Fundamentals and Applications. CRC Press; 2015.

17. Rao R, Chen L, Su J, Cai S, Wang S, Chen Z. Issues and challenges facing aqueous sodium-ion batteries toward practical applications. Battery Energy. 2024;3: 20230036.

18. A comprehensive review of layered transition metal oxide cathodes for sodium-ion batteries: The latest advancements and future perspectives. Materials Science and Engineering: R: Reports. 2025;163: 100902.

19. Whitacre JF, Wiley T, Shanbhag S, Wenzhuo Y, Mohamed A, Chun SE, et al. An aqueous electrolyte, sodium ion functional, large format energy storage device for stationary applications. J Power Sources. 2012;213: 255–264.

20. Zuo W, Qiu J, Liu X, Ren F, Liu H, He H, et al. The stability of P2-layered sodium transition metal oxides in ambient atmospheres. Nature Communications. 2020;11: 3544.

21. Lu Y, Wang L, Cheng J, Goodenough JB. Prussian blue: a new framework of electrode materials for sodium batteries. Chem Commun. 2012;48: 6544–6546.

22. Qian J, Wu C, Cao Y, Ma Z, Huang Y, Ai X, et al. Prussian blue cathode materials for sodium‐ion batteries and other ion batteries. Adv Energy Mater. 2018;8: 1702619.

23. Li D, Liu M, Li W, Fu Q, Wang L, Lai E, et al. Synthesis of Prussian Blue Nanoparticles and Their Antibacterial, Antiinflammation and Antitumor Applications. Pharmaceuticals (Basel). 2022;15. doi:10.3390/ph15070769

24. Gong Z, Yang Y. Recent advances in the research of polyanion-type cathode materials for Li-ion batteries. Energy Environ Sci. 2011;4: 3223–3242.

25. Ni Q, Bai Y, Wu F, Wu C. Polyanion-Type Electrode Materials for Sodium-Ion Batteries. Adv Sci (Weinh). 2017;4: 1600275.

26. Towards high-performance phosphate-based polyanion-type materials for sodium-ion batteries. Energy Storage Materials. 2022;50: 760–782.

27. Ahsan MT, Ali Z, Usman M, Hou Y. Unfolding the structural features of NASICON materials for sodium‐ion full cells. Carbon Energy. 2022;4: 776–819.

28. Bin D, Wang F, Tamirat AG, Suo L, Wang Y, Wang C, et al. Progress in aqueous rechargeable sodium‐ion batteries. Adv Energy Mater. 2018;8: 1703008.

29. Huemer B, Jodlbauer A, Wilkening M, Krenn H, Knoll P, Würschum R, et al. Operando monitoring the redox activity of sodium vanadium titanium phosphate electrodes in organic and aqueous electrolytes by magnetometry. J Mater Chem A. 2025;13: 2934–2942.

30. Zhang H, Tan X, Li H, Passerini S, Huang W. Assessment and progress of polyanionic cathodes in aqueous sodium batteries. Energy Environ Sci. 2021;14: 5788–5800.

31. Hung T-F, Lan W-H, Yeh Y-W, Chang W-S, Yang C-C, Lin J-C. Hydrothermal synthesis of sodium titanium phosphate nanoparticles as efficient anode materials for aqueous sodium-ion batteries. ACS Sustain Chem Eng. 2016;4: 7074–7079.

32. Rational design of functional binder systems for high-energy lithium-based rechargeable batteries. Energy Storage Materials. 2021;35: 353–377.

33. Cholewinski A, Si P, Uceda M, Pope M, Zhao B. Polymer binders: Characterization and development toward aqueous electrode fabrication for sustainability. Polymers (Basel). 2021;13: 631.

34. Chen H, Ling M, Hencz L, Ling HY, Li G, Lin Z, et al. Exploring chemical, mechanical, and electrical functionalities of binders for advanced energy-storage devices. Chem Rev. 2018;118: 8936–8982.

35. Grillet AM, Humplik T, Stirrup EK, Roberts SA, Barringer DA, Snyder CM, et al. Conductivity degradation of polyvinylidene fluoride composite binder during cycling: Measurements and simulations for lithium-ion batteries. J Electrochem Soc. 2016;163: A1859–A1871.

36. Bresser D, Buchholz D, Moretti A, Varzi A, Passerini S. Alternative binders for sustainable electrochemical energy storage – the transition to aqueous electrode processing and bio-derived polymers. Energy Environ Sci. 2018;11: 3096–3127.

37. On the binding mechanism of CMC in Si negative electrodes for Li-ion batteries. Electrochemistry Communications. 2007;9: 2801–2806.

38. Lee J-H, Choi Y-M, Paik U, Park J-G. The effect of carboxymethyl cellulose swelling on the stability of natural graphite particulates in an aqueous medium for lithium ion battery anodes. Journal of Electroceramics. 2006;17: 657–660.

39. Novel polymer Li-ion binder carboxymethyl cellulose derivative enhanced electrochemical performance for Li-ion batteries. Carbohydrate Polymers. 2014;112: 532–538.

40. Effect of high adhesive polyvinyl alcohol binder on the anodes of lithium ion batteries. Electrochemistry Communications. 2011;13: 1051–1053.

41. Wade B. Vinyl Acetal Polymers. Encyclopedia of Polymer Science and Technology. John Wiley & Sons, Ltd; 2016. pp. 1–22.

42. Nguyen FN, Berg JC. The effect of vinyl alcohol content on adhesion performance in poly(vinyl butyral)/glass systems. Journal of Adhesion Science and Technology. 2004 [cited 30 Apr 2025]. doi:10.1163/1568561041257469

43. Olabisi O, Adewale K. Handbook of Thermoplastics. CRC Press; 2016.

44. Bhabhe MD, Galvankar PS, Desai VM, Athawale VD. Copolymers of methyl methacrylate and acrylate comonomers: Synthesis and characterization. J Appl Polym Sci. 1995;56: 485–494.

45. Akin H, Tugut F, Mutaf B, Guney U. Investigation of bonding properties of denture bases to silicone-based soft denture liner immersed in isobutyl methacrylate and 2-hydroxyethyl methacrylate. J Adv Prosthodont. 2014;6: 121–125.

46. Zhang Y-F, Zeng X-R, Ren B-Y. Synthesis and structural characterization of urea–isobutyraldehyde–formaldehyde resins. J Coat Technol Res. 2009;6: 337–344.

47. Two-step synthesis and characterization of urea–isobutyraldehyde–formaldehyde resins. Progress in Organic Coatings. 2009;66: 167–172.

48. Ethylene vinyl acetate-based binder a promising material to produce high power and high energy electrodes with a prolonged cycle life. Solid State Ionics. 2017;301: 15–22.

49. Parvini E, Hajalilou A, Lopes PA, Silva AF, Tiago MSM, Fernandes PMP, et al. 3R Batteries: Resilient, Repairable, and Recyclable Based on Liquid Gallium Electrode. Advanced Materials Technologies. 2024;9: 2301189.

50. Rodrigo JL, Carrasco P, Alamo J. Thermal expansion of NaTi2(PO4)3 studied by rietveld method from X-ray diffraction data. Mater Res Bull. 1989;24: 611–618.

51. Bamgbelu L, Holt KB. In Situ Determination of pH at Nanostructured Carbon Electrodes Using IR Spectroscopy. Materials. 2019;12: 4044.

52. Liu M, Wang Y, Wu Y, Wan H. Hydrolysis and recycling of urea formaldehyde resin residues. J Hazard Mater. 2018;355: 96–103.

53. Hirata Y, Marais S, Nguyen Q, Cabot C, Sauvage J. Relationship between the gas and liquid water permeabilities and membrane structure in homogeneous and pseudo-bilayer membranes based on partially hydrolyzed poly(ethylene-co-vinyl acetate). J Memb Sci. 2005. doi:10.1016/j.memsci.2005.01.002

54. Pilipavičius J, Traškina N, Juodkazytė J, Vilčiauskas L. The mechanism of NaTi2(PO4)3 aqueous electrochemical degradation revisited. Electrochim Acta. 2023;465: 142993.

55. du Baret de Limé A, Lein T, Maletti S, Schmal K, Reuber S, Heubner C, et al. Impact of electrode defects on battery cell performance: A review. Batter Supercaps. 2022;5. doi:10.1002/batt.202200239

SANTRAUKA

Šiame darbe buvo tiriami polimerai ir iš jų pagaminti kompozitiniai elektrodai vandeninėms natrio jonų baterijoms. Polimerų adhezinės savybės buvo tiriamos patalpinant polimerais ir jų kompozitais užteptų s metalinius diskus į elektrolitų tirpalus su neutraliais ir rūgštiniais pH. Tyrimo metu nustatyti trys geriausiai pasirodžius medžiagos (PVB, PGPQ bei PB67) buvo toliau tiriamos kaip rišikliai NTP bei NVTP elektroduose ir palyginti su įprastai naudojamu PVDF. CV parodė, jog polimerai nėra elektrochemiškai aktyvūs, tuo tarpu galvanostatinis ciklavimas parodė jog NTP elektroduose ant tinkleliu PVDF turinčio kompozito talpa siekė 90 mAh/g ir po ciklavimo išlaikė 67,97% pradinės talpos, tuo tarpu PVB parodė 105 mAh/g ir išlaikė 41%, PGPQ – 101 mA/g ir 52.18%, PB67- 84 mAh/g ir 53.59%. Ciklavimai taip pat buvo atlikti naudojant elektrodus teptus ant plieninės folijos, kur dėl prastos adhezijos PVDF bei PB67 turintys elektrodai nuėjo nuo paviršiaus, tuo tarpu PVB bei PGPQ elektrodai parodė 96 mAh/g bei 82 mAh/g pradines talpas bei 24,63 bei 30,84% talpas po 300 cikl7 atitinkamai. Identi6ki tyrimai buvo atlikti ir su NVTP elektrodais naudojant tuos pa2ius pasirinktus rišiklius ir įspaustuose į tinklelius elektroduose buvo gautos panašios apie 40 mAh/g siekiančios talpas, ant folijos tepti elektrodai elgėsi panašiai kaip ir NTP atveju su PVB išimtimi, kur dalis elektrodo atšoko nuo paviršiaus cikluojant ir dėl to drastiškai sumažėjo elektrodo talpa. Elektrodų paviršiai prieš ir po ciklavimo buvo ištirti panaudojant SEM. Nuotraukos parodė jog PVDF elektrodai po ciklavimo turėjo daug plyšių ant paviršiaus, PVB šiek tiek mažiau, o PGPQ mažiausiai. Išanalizavus šiuos duomenis PGPQ buvo išrinktas kaip optimalus rišiklis kompozitinėms vandeninėms natrio jonų baterijoms.

Annex

1a)

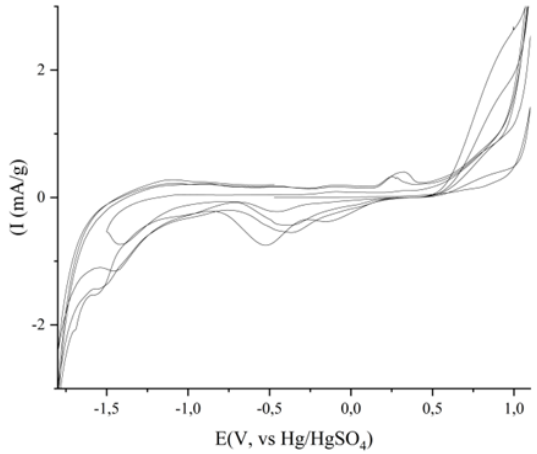

1b)

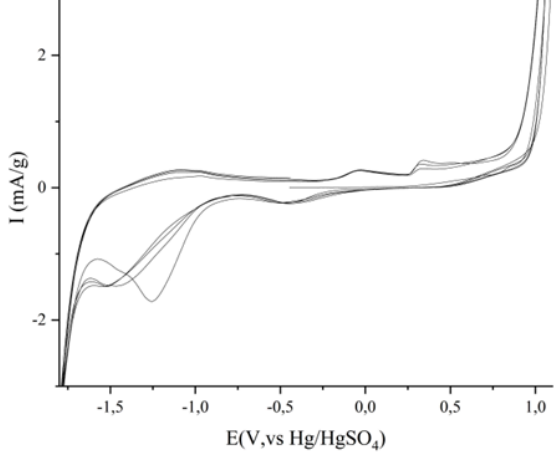

1c)

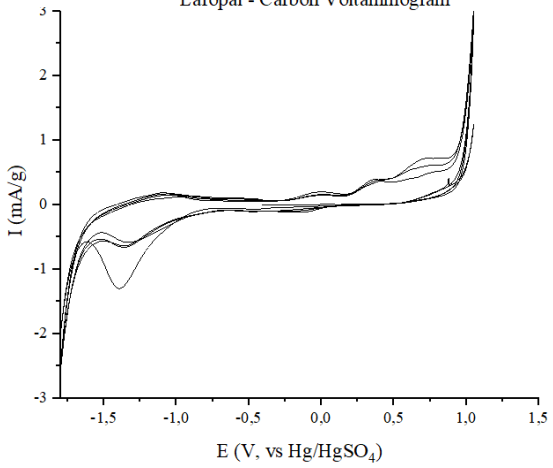

1d)

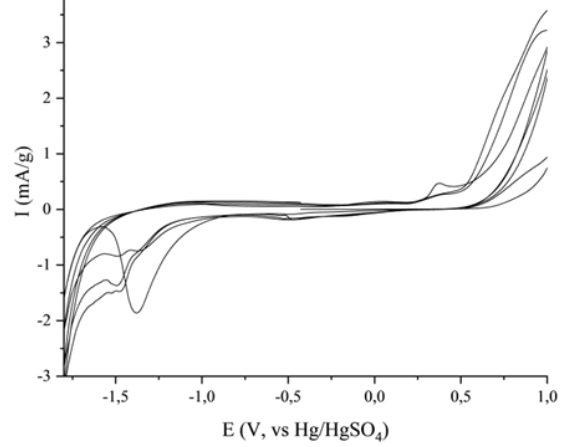

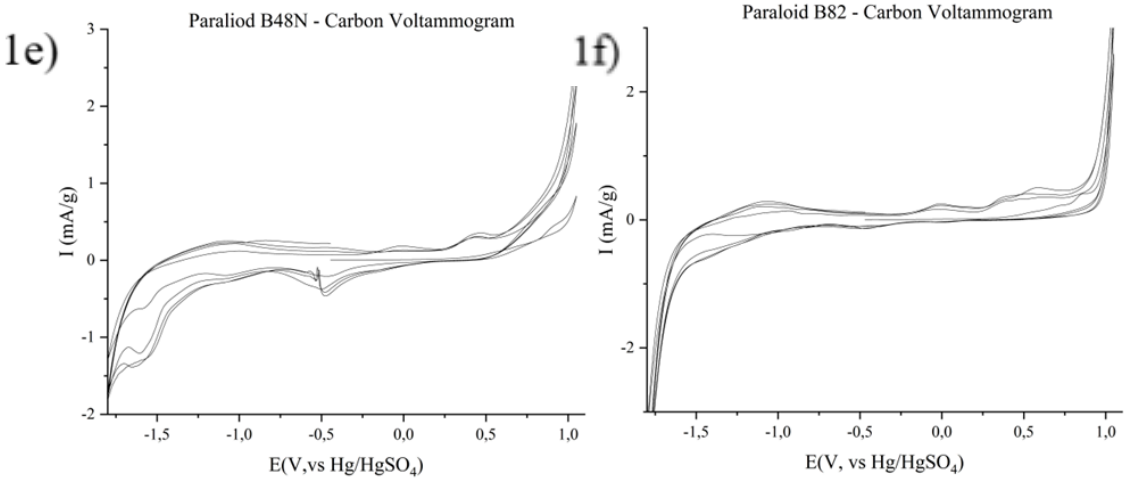
1e)
Paraliod B48N - Carbon Voltammogram
I (mA/g)
E(V,vs Hg/HgSO4)
1f)
Paraloid B82 - Carbon Voltammogram
I (mA/g)
E(V, vs Hg/HgSO4)

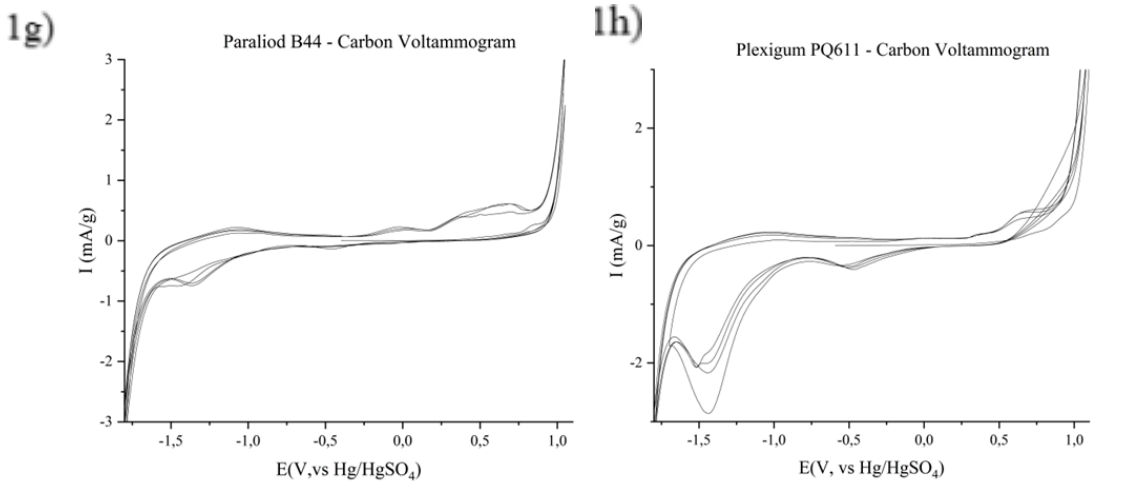
1g)
Paraliod B44 - Carbon Voltammogram
I (mA/g)
E(V,vs Hg/HgSO4)
1h)
Plexigum PQ611 - Carbon Voltammogram
I (mA/g)
E(V, vs Hg/HgSO4)

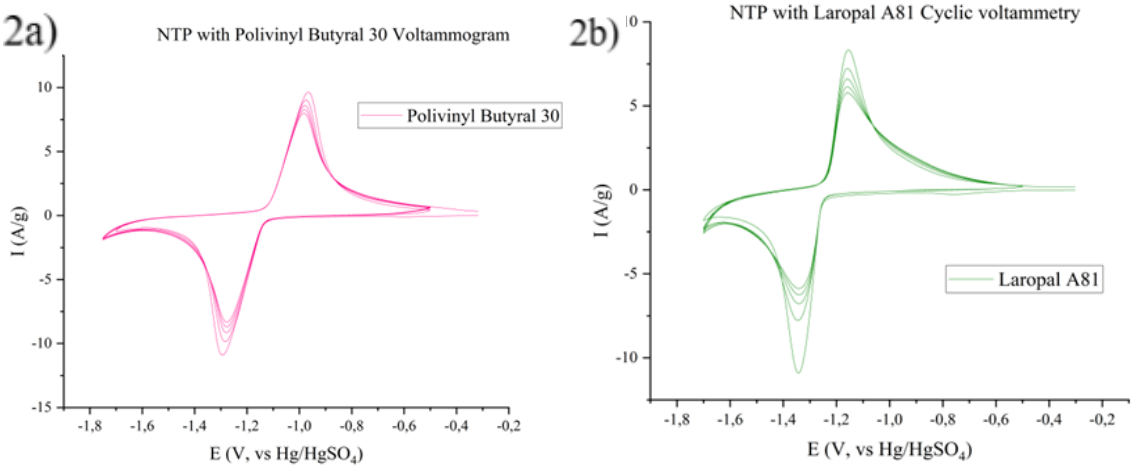
2a)
NTP with Polivinyl Butyral 30 Voltammogram
Polivinyl Butyral 30
I (A/g)
E (V, vs Hg/HgSO4)
2b)
NTP with Laropal A81 Cyclic voltammetry
Laropal A81
I (A/g)
E (V, vs Hg/HgSO4)

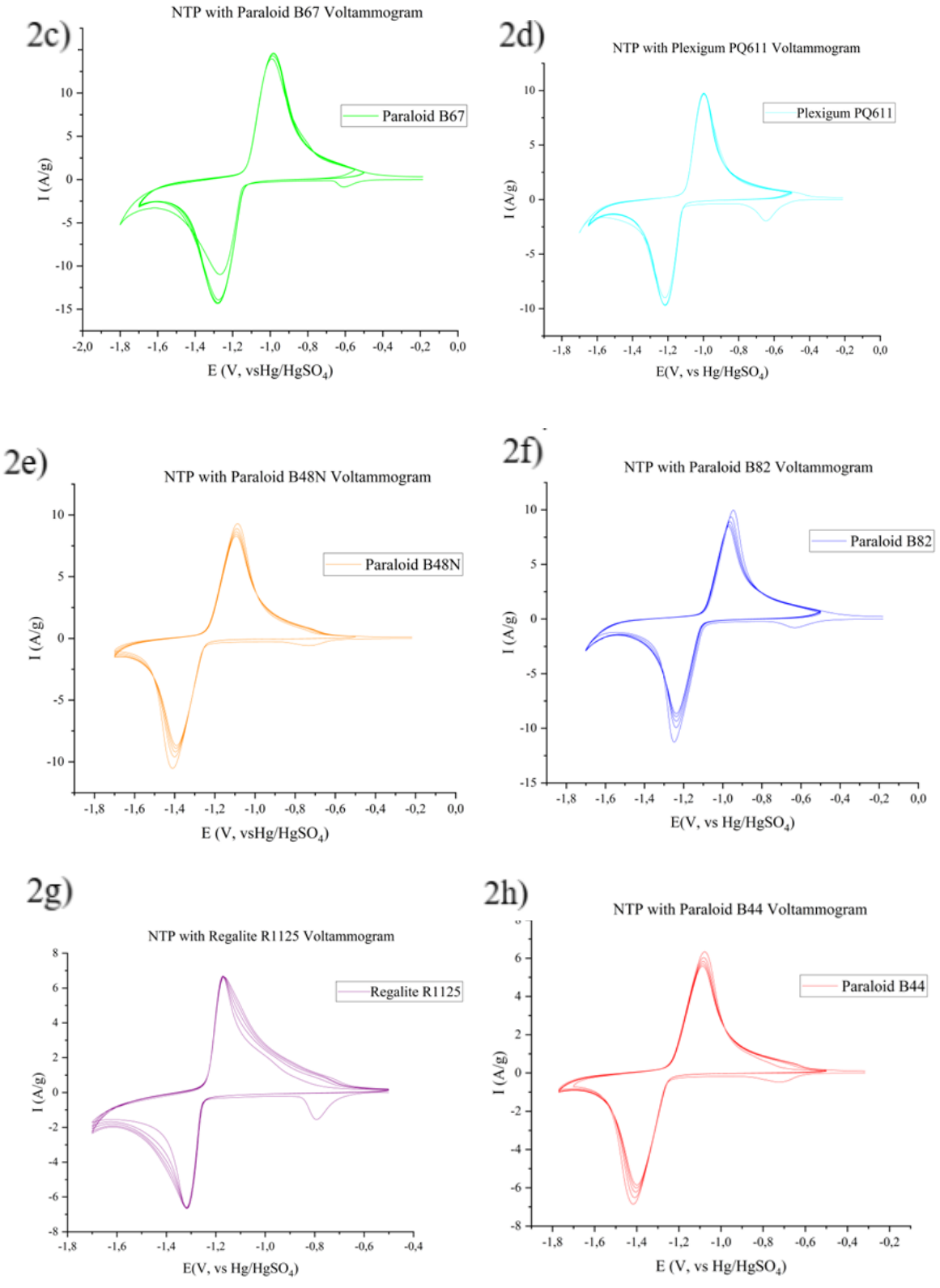

Cyclic voltammograms of 1a) PVB-CB; 1b) PB67-CB; 1c) LA81-CB; 1d)RR1125-CB; 1e) PB48N-CB; 1f) PB82-CB; 1g) PB44-CB; 1h) PGPQ-CB; 2a) NTP-PVB; 2b) NTP-LA81; 2c) NTP-PB67; 2d) NTP-PGPQ; 2e) NTP-PB48N; 2f) NTP-PB82; 2g) NTP-RR1125; 2h) NTP- PB44.

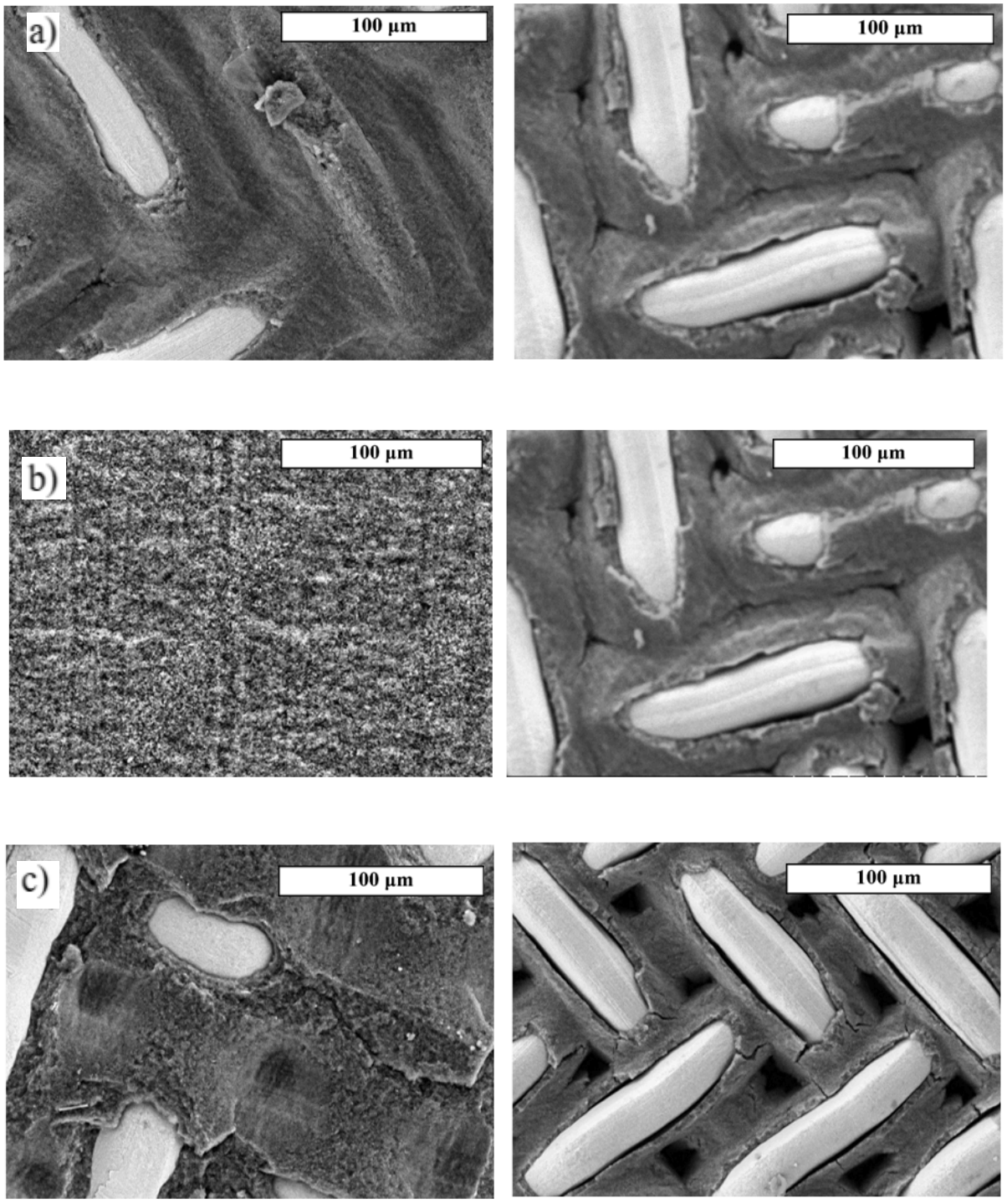
a)
100 µm
100 µm
b)
100 µm
100 µm
c)
100 µm
100 µm

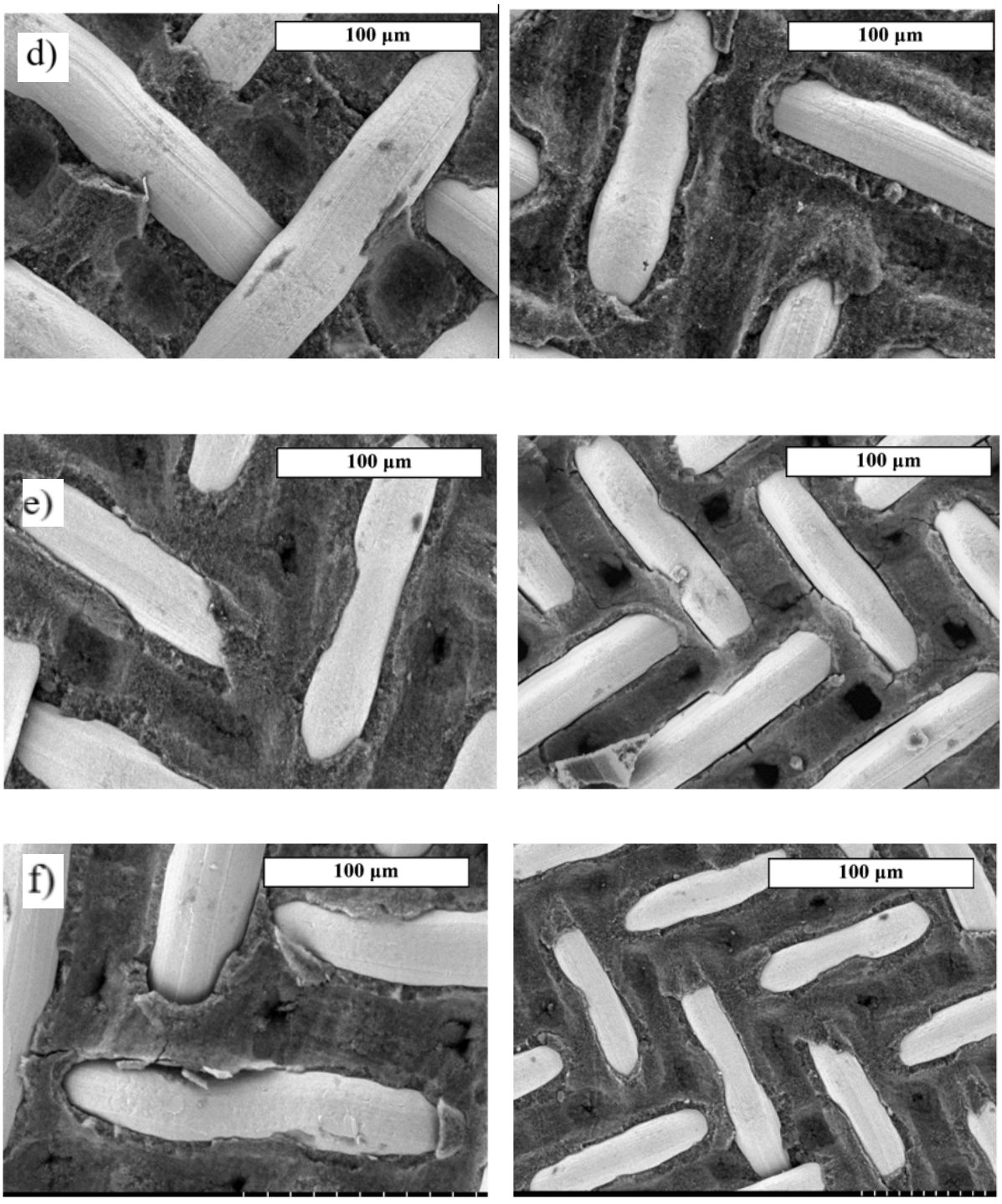

SEM images of: a) NTP-PVB, b) NVTP-PVB, c)PGPQ-NTP, d) PGPQ-NVTP, e)PB67-NTP, f)PB67-NVTP electrodes pressed on mesh pre galvanic cycling (on the left) and post galvanic cycling (on the right).